

612-1917
[REDACTED]
Copies [REDACTED]

LAUNCH VEHICLE ERROR ANALYSIS
FOR APOLLO/SATURN 204 [REDACTED]

DECEMBER 15, 1966

[REDACTED]
[REDACTED]
[REDACTED]

THIS DOCUMENT CONTAINS INFORMATION AFFECTING
THE NATIONAL DEFENSE OF THE UNITED STATES
WITHIN THE MEANING OF THE ESPIONAGE LAWS, TITLE
18 U. S. C., SECTIONS 793 AND 794. ITS DISSEMINATION
OR THE REVELATION OF ITS CONTENTS IN ANY MANNER
TO AN UNAUTHORIZED PERSON IS PROHIBITED BY LAW.

[REDACTED]
Prepared by Bell Telephone Laboratories, Incorporated
on behalf of Bellcomm, Inc.
[REDACTED]

[REDACTED]

TABLE OF CONTENTS

	<u>Page</u>
I. Introduction	1
II. Reference Trajectory Description	3
III. Simulation Description	6
A. Missile Dynamics	6
B. Inertial Platform Simulation	9
C. Accelerometer Processing	11
D. Navigation Equations	12
E. Guidance Equations	12
IV. Vehicle Data	14
V. Error Analysis Results	17
A. Errors at S-IVB Cutoff	17
B. Errors at 640 Seconds	19
VI. Analytical Investigations	32
A. Noise Models	32
B. Noise and Dynamic Response of the M/F Filter	34
C. Noise Response of the Navigation Equations	38
D. The Effect of Noise on the Prediction of the Cutoff Time	42
References	
Appendix	
Figures 1-13	

Ref. No. 66 611
Copy No. of Copies

I. Introduction

This report describes an error analysis of the Apollo/Saturn 204 test mission launch vehicle trajectory. The purpose of this study was to evaluate uncertainties at launch vehicle cutoff due to inertial platform and performance uncertainties. The study was performed by the Control Systems Analysis Department at Bell Telephone Laboratories, Incorporated on behalf of Bellcomm, Inc.

The AS-204 mission is a manned orbital flight designed to test spacecraft operations and launch vehicle systems performance for an orbital mission. The launch vehicle for AS-204, consisting of an S-IB first stage and an S-IVB second stage, will be launched from Launch Complex 34 at Cape Kennedy along a flight azimuth of 72 degrees. In this study, the SA-204 Launch Vehicle Operational Flight Trajectory document¹ was used as a reference for both vehicle data and the nominal trajectory description.

The effects of platform and performance uncertainties are determined by simulating perturbed trajectories for $\pm 3\sigma$ magnitudes of each error source. The resulting 3σ variations in significant trajectory parameters are determined both at S-IVB cutoff and at a fixed time (50 seconds) after nominal S-IVB cutoff. In addition, three analytical

This document contains information affecting the national defense of the United States within the meaning of the Espionage Laws, Title 18 U.S.C. Sec. 793 and 794. Its transmission or the revelation of its contents in any manner to an unauthorized person is prohibited by law.

investigations were performed. These include:

- (1) Noise and dynamic response of the M/F filter.
- (2) Noise response of the navigation equations.
- (3) The effect of noise on the prediction of cutoff time.

The noise source considered in these studies is the accelerometer measurement quantization.

Using three-sigma platform and performance uncertainties obtained from references 10 and 11, the following are the three-sigma deviations in the actual state at S-IVB cutoff:

Radius	1492.6 ft
Velocity magnitude	3.981 ft/sec
Flight path angle	.0131 deg
Inclination	.0068 deg
Node angle	.0252 deg
Time from launch	19.217 sec
S-IVB fuel reserve	1579.5 lbs

II. Reference Trajectory Description

The nominal closed loop trajectory used for this study is a match of the SA-204 Launch Vehicle Operational Flight Trajectory.¹ To develop this nominal trajectory, an open loop trajectory was first generated which matches the significant parameters on the reference.

The pitch profile of the open loop trajectory consists of a 10 second vertical rise followed by an instantaneous change in pitch (kick angle) to initiate a gravity turn. The gravity turn is flown until 133 seconds at which time the attitude is fixed. At 185.4 seconds, the vehicle is given a second instantaneous pitch change followed by a constant pitch rate until S-IVB cutoff.

The kick angle at 10 seconds was selected to match the reference altitude at 185.4 seconds (321,405 ft). The pitch angle at 185.4 seconds together with the constant pitch rate and S-IVB cutoff time were chosen to satisfy the radius (21,442,123 ft), velocity (25,702.53 ft/sec), and inertial flight path angle (0.0 deg.) at S-IVB cutoff. These constraints, together with a launch azimuth of 72 degrees and no roll or yaw maneuvers, yield an orbital plane with an inclination of 32.469 degrees and an angle from the launch meridian to the descending node of 123.315 degrees.

The resulting open loop reference trajectory was then processed to calculate all required guidance constants. A complete closed loop simulation was then performed, using the 2-stage IGM equations, to generate the nominal trajectory shown in Table 1.

TABLE 1

Closed Loop Reference Trajectory

<u>Event</u>	<u>Time</u>	<u>Latitude</u>	<u>Longitude</u>	<u>Altitude</u>	<u>Velocity</u>	<u>Flight Path Angle</u>	<u>Flight Path Azimuth</u>
	sec	deg	deg	ft	ft/sec	deg	deg
LAUNCH	0	28.36	-80.56	40.	1341.76	0.	90.02
IEC Ø	141.65	28.52	-79.99	189762.	7586.15	25.91	75.83
SI Ø FF	144.60	28.54	-79.94	199591.	7753.06	25.52	75.77
S4 Ø N	149.00	28.56	-79.87	214027.	7693.78	24.67	75.81
MIX1	153.50	28.58	-79.79	228322.	7730.06	23.91	75.82
JETISG	157.20	28.60	-79.73	239822.	7771.96	23.30	75.83
JETLES	185.40	28.73	-79.22	320557.	8143.38	18.98	75.88
MIX2	475.00	30.78	-69.94	578143.	18183.15	-1.23	79.38
S4 Ø FF1	589.495	31.79	-62.79	536098.	25702.64	0.	83.01

III. Simulation Description

The simulation required for the error analysis was performed using the Bellcomm Apollo Simulation Program (BCMASP).² This program is a three degree of freedom simulator which generates the trajectory by numerical integration of all significant accelerations acting on the vehicle. Since BCMASP is described elsewhere in detail,^{3,4} only those aspects of the program that relate directly to the error analysis will be discussed in this report.

A functional diagram of the calculations performed in each guidance cycle by the simulation program is given in Figure 1. As illustrated in this diagram, the missile dynamics are simulated to obtain the actual position, velocity, and the integral of the nongravity acceleration. The accelerometer measurements are simulated by converting the integral of nongravity acceleration to platform coordinates and adding errors associated with the platform gyros and accelerometers. The accelerometer processing, navigation, and guidance equations are equivalent to those specified in the Launch Vehicle Digital Computer (LVDC) Equation Defining Document for AS-204.⁵ The pertinent details of these functions will now be discussed.

A. Missile Dynamics

In simulating the missile dynamics, the accelerations due to thrust, drag, lift, and gravity were considered.

Second stage thrust and mass flow rates for both stages were assumed constant. The first stage thrust was determined by the following equation:

$$T = T_{sl} + A_t(p_o - p)$$

where

T = thrust

T_{sl} = the constant sea level thrust

A_t = thrust chamber area

p = atmospheric pressure

p_o = sea level pressure

Thrust buildup and decay were simulated by an equivalent lengthening of the burn at full thrust.

The thrust levels and mass flow rates were chosen by the following procedure with the intention of matching position and velocity along the reference trajectory:¹

1. The event times shown in Table 1 were selected to reflect the effect of thrust buildups and decays.
2. Constant mass flow rates were computed such that the vehicle weight at the events matched the reference.

3. T_{sl} and A_t were adjusted such that the velocity magnitude and inertial flight path angle matched the reference at the time of jettisoning the launch escape system.
4. S-IVB thrust at 5.0:1 mixture ratio was assumed nominal, at 5.5:1 mixture ratio, an average thrust from the reference was used, and at 4.7:1 mixture ratio, the thrust was adjusted to achieve cutoff velocity at the proper time.

Drag and lift forces were computed using the drag and lift coefficient curves given in reference 1 and the Patrick Reference Atmosphere.⁶ In computing the normal force, the torque created by the lift force is balanced by deflecting the thrust vector from the roll axis. The gravitational force is computed from the standard Fisher Ellipsoid model of the Earth as defined in reference 7.

The attitude of the vehicle is determined by integrating constant attitude rates. These rates are recomputed each guidance cycle and ordered to accomplish the required change in attitude as determined by the guidance equations. Although angular dynamics and autopilot response are not simulated, rate limiting of 1 degree/second is applied.

~~CONFIDENTIAL~~

B. Inertial Platform Simulation

The accelerometer measurements are simulated by integrating the actual sensed acceleration due to thrust and aerodynamic forces, and adding errors associated with the platform gyros and accelerometers. The error sources considered include the following:

- (1) initial platform misalignment
- (2) gyro drift
- (3) gyro mass unbalance
- (4) gyro anisoelastic effects
- (5) accelerometer misalignment
- (6) accelerometer bias
- (7) accelerometer scale factor error
- (8) accelerometer measurement quantum size

The inertial platform alignment and the orientation of the gyro axes are illustrated in Figure 2. As shown in Figure 3, the operations performed to simulate this platform proceed by first forming the increment in velocity gained during the last guidance cycle due to thrust and aerodynamic forces. This velocity increment ($\overline{\Delta V}_a$) is expressed in the platform coordinate system which is defined by the nominal platform alignment at guidance reference release.

~~CONFIDENTIAL~~

~~CONFIDENTIAL~~

The effects of initial misalignment and platform drift are simulated by the A matrix. This matrix relates the actual instantaneous platform orientation to the nominal alignment. The initial misalignment is described by three Euler angles taken about the pitch, yaw, and roll axes. The drift rate about each platform axis is given by

$$\omega_j = GD_j + U_{sj}a_{ij} + U_{ij}a_{sj} + U_{oj}a_{oj} + S_j a_{ij}a_{sj}$$

where

GD_j = the fixed gyro drift rate of the j^{th} axis gyro

U_{sj}, U_{ij}, U_{oj} = the mass unbalance about the spin, input, and output axes of the j^{th} axis gyro

S_j = the anisoelastic constant of the j^{th} axis gyro, and

a_{ij}, a_{sj}, a_{oj} = the sensed acceleration along the input, spin, and output axes of the j^{th} axis gyro.

The total drift rate is calculated and used to update the A matrix each computation cycle.

With reference to Figure 3, the B matrix simulates accelerometer misalignment. Since this matrix is not time dependent, it need only be calculated once and is given by

$$[B] = \begin{bmatrix} \cos \epsilon_{yx} \cos \epsilon_{xz} & -\sin \epsilon_{xy} \cos \epsilon_{yz} & \sin \epsilon_{xz} \cos \epsilon_{xy} \\ \sin \epsilon_{yx} \cos \epsilon_{yz} & \cos \epsilon_{yx} \cos \epsilon_{yz} & -\sin \epsilon_{yz} \cos \epsilon_{yx} \\ -\sin \epsilon_{zx} \cos \epsilon_{zy} & \sin \epsilon_{zy} \cos \epsilon_{zx} & \cos \epsilon_{zx} \cos \epsilon_{zy} \end{bmatrix}$$

where the epsilons are the angles by which the accelerometer axes deviate from the platform axes as illustrated in Figure 4. Accelerometer bias and scale factor error are introduced by the vector $\overline{a_b}$ and the matrix $[1 + SF]$ respectively. The scale factor matrix is of the form

$$\begin{bmatrix} (1 + SF_x) & 0 & 0 \\ 0 & (1 + SF_y) & 0 \\ 0 & 0 & (1 + SF_z) \end{bmatrix}$$

where SF_i represents the scale factor error of the accelerometer along the i^{th} axis.

$\overline{\Delta V_m}$, the output of the platform simulation, now represents the change in the accelerometer measurements that has occurred during the last computation cycle. This quantity is used by the navigation equations, the M/F filter, and the mixture ratio shift sensor.

C. Accelerometer Processing

The accelerometer processing program simulates two significant functions: the mixture ratio shift sensor and the M/F filter. In Section VI.B, the M/F filter specified

in reference 8 is shown to provide an unbiased estimate of the mass intercept time ($\hat{\tau}$) given by

$$\hat{\tau} = (M/F)^S V_{ex}$$

where $(M/F)^S$ is the output of the M/F filter and V_{ex} is the effective exhaust velocity. The mass intercept time is used by the guidance equations to predict the vehicle's acceleration.

D. Navigation Equations

The onboard navigation was simulated by using the accelerometer measurements in the MIT "Average G" equations. These equations were used because they are simpler in form and are demonstrably equivalent⁹ to the "Boost Navigation" equations in the LVDC Equation Defining Document.⁵ The gravity model used was taken directly from the "Boost Navigation" section of the LVDC document.

E. Guidance Equations

There are two phases of guidance for the AS-204 launch vehicle. During the atmospheric portion of flight, the vehicle attitude is commanded to follow a specified pitch program. This program commands a vertical attitude for 10 seconds, at which time the attitude is ordered to follow a sixth order pitch polynomial. At 133 seconds, the

attitude is again held constant until active guidance takes command at 185.4 seconds. The coefficients of the sixth order polynomial were calculated by a least squares fit to the gravity turn portion of the open loop reference trajectory which was generated with BCMASP.

After 185.4 seconds, the vehicle is guided by the 2-stage IGM equations described in the LVDC Equation Defining Document.⁵ IGM operates in its normal mode until time to go reaches 46 seconds. At this time, the \tilde{X} mode is entered and thereafter IGM controls only the velocity vector at cutoff. When time to go reaches 14 seconds, the last steering orders computed by the IGM equations are flown without updating and a parabolic extrapolation for cutoff time based on velocity is employed.

IV. Vehicle Data

Tables 2 and 3 present the vehicle data used in the error analysis trajectory simulation. Table 2 lists the engine performance data as discussed in section III - A. The weight summary, presented in Table 3, is derived from the Operational Flight Trajectory.¹

TABLE 2
Engine Performance Data

S-IB Engine Performance Data

Sea level thrust	1710486. lbs
Weight rate	6226.655 lbs/sec
Thrust chamber area	6638.749 in ²
Drag area	360. ft ²

S-IVB Engine Performance Data

5.0:1 Mixture Ratio

Thrust	200000. lbs
Weight rate	504.724 lbs/sec

5.5:1 Mixture Ratio

Thrust	226200. lbs
Weight rate	534.6 lbs/sec

4.7:1 Mixture Ratio

Thrust	190220. lbs
Weight rate	441.728 lbs/sec

TABLE 3
Weight Summary

Inert wgt at cutoff	65,070	
Fuel reserve at cutoff	4,062	
Injection weight		69,132
S-IVB weight consumed	224,681	
Launch escape system	8,500	
Ullage cases	220	
S-IVB weight at separation		302,533
S-IB weight consumed	891,190	
S-IB inert weight	102,645	
Vehicle liftoff weight		1,296,368

V. Error Analysis Results

The error analysis results corresponding to three-sigma values of platform and performance errors are compiled in this section. The platform uncertainties were derived from reference 10, and the performance uncertainties were obtained from reference 11.

A. Errors at S-IVB Cutoff

Tables 4 through 7 present the errors at S-IVB cutoff that were generated by simulating perturbed closed loop trajectories for each error source. The tabulated differences represent the actual state on the perturbed trajectory minus the actual state on the nominal. Definitions of all symbols are listed in the Appendix.

In computing the root-sum-square (RSS) values, the larger of the differences obtained from the positive and negative perturbation of each error source was used. The RSS values represent the three-sigma magnitudes of variations in the parameters at cutoff.

Total three-sigma values, considering both platform and performance uncertainties, are listed below for the significant parameters at S-IVB cutoff.

Radius	1492.6 ft
Velocity magnitude	3.981 ft/sec
Flight path angle	.0131 deg

Inclination	.0068 deg
Node angle	.0252 deg
Time from launch	19.217 sec
S-IVB fuel reserve	1579.5 lbs

The velocity magnitude uncertainty shown above also includes the effects of quantization on the cutoff time computation (section VI D) and a .03 second three-sigma uncertainty in the cutoff execution. The cutoff execution uncertainty contributes 2.61 ft/sec as computed from

$$\Delta V \approx a_T \cos \alpha \Delta t$$

where a_T is the axial acceleration (88.6 ft/sec²) and α is the angle of attack (11 deg) at S-IVB cutoff.

Figures 5 and 6 show S-IVB fuel reserve as a function of S-IB and S-IVB fuel loading respectively. The figures indicate that the fuel reserve could be increased by loading additional fuel in both stages.

Fuel optimization for the zero lift trajectory was investigated. In Section II, it was noted that the gravity turn was selected to match the altitude of the MSFC trajectory at 185.40 seconds. Figure 7 demonstrates that the S-IVB cutoff time could be decreased by .5 seconds by reshaping the trajectory. Since this results in a fuel saving of only

220 lbs, the MSFC reference trajectory is a near optimum zero lift trajectory. (Lifting trajectories may add to the fuel reserve,¹³ but were not considered in this report.)

The uncertainty in fuel reserve is controlled by variations in first and second stage I_{sp} (no mass rate change). For the assumed three-sigma I_{sp} variation of 1%, the probability of fuel depletion is extremely small. Figures 12 and 13 are graphs showing the variation of the three-sigma fuel reserve and the probability of fuel depletion with changes in the assumed value of I_{sp} uncertainties and nominal fuel reserve.

B. Errors at 640 Seconds

Tables 8 through 11 present the errors in local vertical coordinates at 640 seconds, approximately 50 seconds after nominal S-IVB cutoff. This coordinate system and all symbols are defined in the Appendix. The values tabulated in Tables 8 and 9 represent differences in the actual state (perturbed-nominal), whereas those tabulated in Tables 10 and 11 represent differences in the estimated state (perturbed-nominal) as determined by the onboard launch vehicle navigation equations.

The errors are presented in this form to provide data for generating transition matrices between fixed times on the AS-204 trajectory.

ITAL

TABLE 4
ERRORS AT S-IVB CUTOFF DUE TO PLATFORM ERRORS

DIFFERENCE IN	XDOT FT/SEC	YDOT FT/SEC	ZDOT FT/SEC	X FT	Y FT	Z FT	T SEC
GDSVX ± .100	0,001	0,003	0,472	0,1	0,5	244,7	0,0000
GDSVY ± .100	0,001	-0,001	-0,473	0,3	-0,2	-244,7	0,0000
GDSVZ ± .075	0,000	-0,002	-3,062	0,3	-0,2	-495,2	0,0000
GDSVX ± .075	-0,000	0,004	3,061	-0,2	0,	495,3	-0,0000
GDSVZ ± .075	-0,304	3,316	0,002	-173,9	525,2	0,4	-0,0003
GDSVX ± .075	0,304	-3,313	-0,002	174,1	-524,5	-0,3	0,0003
USSVX ± .100	0,003	0,001	0,364	0,9	-0,5	196,5	0,0000
USSVY ± .100	0,002	-0,000	-0,364	0,6	-0,5	-196,6	0,0000
USSVZ ± .075	-0,001	-0,003	-2,485	-0,2	-1,0	-524,4	-0,0000
USSVX ± .075	0,002	0,004	2,484	0,2	-0,2	524,4	0,0000
USSVZ ± .100	0,001	0,001	-0,000	0,2	-0,5	-0,0	0,0000
UISVX ± .100	0,001	-0,000	-0,000	0,4	-0,5	0,1	0,0000
UISVY ± .100	0,001	0,000	0,000	0,4	-0,2	0,1	0,0000
UISVZ ± .075	0,000	0,001	-0,000	0,1	-0,2	-0,1	0,0000
UISVX ± .075	0,002	-0,000	-0,001	0,4	-0,5	-0,1	0,0000
UISVY ± .075	0,003	-0,000	0,000	0,7	-0,5	0,1	0,0000
UISVZ ± .075	-0,220	3,678	0,002	-140,7	531,7	0,2	-0,0000
UOSVX ± .060	0,221	-3,675	-0,002	141,3	-530,5	-0,2	0,0001
UOSVY ± .060	-0,001	0,003	0,416	-0,5	-0,2	202,5	-0,0000
UOSVZ ± .060	0,001	-0,001	-0,416	0,6	0,	-202,5	0,0000
UOSVX ± .060	0,001	-0,002	-2,743	0,2	-0,7	-402,3	0,0000
UOSVY ± .060	0,001	0,002	2,743	0,2	-0,2	402,3	0,0000
UOSVZ ± .060	-0,368	2,236	0,002	-192,3	452,0	0,4	-0,0003
SSVX ± .050	0,370	-2,235	-0,002	192,9	-451,5	-0,4	0,0004
SSVY ± .050	0,000	0,001	-0,000	0,	-0,2	0,1	0,
SSVZ ± .050	0,002	0,001	-0,000	0,7	0,2	0,0	0,0000
SSVX ± .050	0,001	0,000	-0,001	0,2	-0,5	-0,1	0,0000
SSVY ± .050	0,002	0,000	0,001	0,3	-0,7	0,2	0,0000
SSVZ ± .050	0,000	0,001	0,000	0,2	0,2	0,0	0,0000
SFSVX ± .00003	0,001	-0,000	-0,000	0,4	-0,5	0,1	0,0000
SFSVY ± .00003	-0,694	0,021	0,000	-211,7	6,7	-0,4	-0,0094
SFSVZ ± .00003	0,695	-0,020	-0,000	211,6	-9,0	0,5	0,0094

COM DIFFERENCE IN

SFSVY = ,00003	XDOT FT/SEC	YDOT FT/SEC	ZDOT FT/SEC	X FT	Y FT	Z FT	T SEC
SFSVZ = ,00003	-0,025	-0,407	-0,001	-6,5	-161,2	-0,3	-0,0027
ABSVX = ,00003	0,028	0,412	0,001	7,3	164,2	0,2	0,0028
ABSVY = ,00003	0,000	0,001	-0,000	0,1	-0,2	-0,0	0,
ABSVZ = ,00003	0,	0,001	0,000	0,1	0,2	0,1	0,
CHI1X = ,00196	-0,528	-0,025	-0,000	-158,9	-4,0	0,1	-0,0072
CHI1Y = ,00573	0,528	0,027	0,000	159,1	3,2	0,1	0,0072
CHI1Z = ,00196	-0,019	-0,641	-0,001	-4,9	-176,5	-0,2	-0,0024
EPSVXY = ,00834	0,021	0,648	0,001	5,4	180,2	0,2	0,0025
EPSVYZ = ,00278	0,001	-0,001	-0,509	0,4	0,	-158,9	0,0000
EPSVZX = ,00879	0,001	0,002	0,508	0,3	-0,2	159,0	0,0000
EPSVZY = ,00834	0,001	0,002	0,295	0,1	-0,2	159,1	0,0000
RSS	0,002	-0,002	-0,295	0,8	0,2	-158,9	0,0000
	0,001	-0,004	-2,349	0,6	-1,0	-585,9	0,0000
	0,003	0,004	2,349	0,7	0,	586,0	0,0000
	-0,275	0,912	0,001	-138,9	214,2	-0,5	-0,0008
	0,282	-0,909	-0,001	141,1	-211,2	0,3	0,0010
	1,387	0,443	0,006	414,7	96,5	-3,2	0,0200
	-1,385	-0,441	-0,006	-413,6	-96,7	3,0	-0,0199
	0,000	0,000	-0,000	0,1	-0,2	0,1	0,
	0,002	0,000	-0,000	0,9	0,	-0,1	0,0000
	-0,070	-3,907	-0,006	-11,7	-931,5	-0,8	-0,0114
	0,073	3,911	0,006	12,5	931,7	0,7	0,0114
	0,002	-0,000	-0,000	0,8	0,2	-0,1	0,0000
	0,001	0,000	-0,000	0,3	-0,5	0,1	0,0000
	0,004	0,007	3,411	0,9	1,0	882,5	0,0000
	-0,003	-0,005	-3,411	-0,1	-0,5	-882,3	0,
	-0,001	-0,006	-1,277	0,1	-1,2	-677,4	0,
	0,001	0,008	1,277	-0,1	0,5	677,5	0,0000
	1,746	6,815	6,537	591,5	1321,3	1566,4	0,0262

TABLE 5
ERRORS AT S-IVB CUTOFF DUE TO PLATFORM ERRORS

DIFFERENCE IN	R FT	BETA E-3 DEG	WGT LB	PHIT E-3 DEG	V FT/SEC	GINCL E-3 DEG	DNODE E-3 DEG
GDSVX = .100	3,7	0,0	-0,0	0,0	0,005	-0,8	-1,7
GDSVY = .100	-3,2	-0,0	-0,0	-0,0	-0,004	0,8	1,7
GDSVZ = .075	-6,5	-0,1	-0,0	-0,0	-0,034	2,6	12,0
GDSVZ = .075	6,5	0,1	0,0	0,0	0,034	-2,6	-12,0
GDSVZ = .075	447,2	6,0	0,1	-0,9	-1,302	0,0	0,1
GDSVZ = .075	-446,0	-6,0	-0,1	0,9	1,301	-0,0	-0,1
USSVX = .100	2,5	0,0	-0,0	0,0	0,007	-0,7	-1,3
USSVY = .100	-2,7	-0,0	-0,0	-0,0	-0,002	0,7	1,3
USSVY = .075	-7,5	-0,1	0,0	-0,0	-0,028	2,4	9,6
USSVZ = .075	6,7	0,1	-0,0	0,0	0,029	-2,4	-9,6
USSVZ = .100	0,0	0,0	-0,0	0,0	0,001	0,0	0,0
UISVX = .100	0,0	0,0	-0,0	0,0	0,001	0,0	0,0
UISVY = .100	0,0	0,0	-0,0	0,0	0,001	-0,0	-0,0
UISVY = .075	-0,2	0,0	-0,0	0,0	0,002	0,0	0,0
UISVZ = .075	0,0	0,0	-0,0	0,0	0,002	0,0	0,0
UISVZ = .075	463,5	6,9	0,0	-0,8	-1,338	0,0	0,1
UOSVX = .060	-461,7	-6,9	-0,0	0,8	1,338	-0,0	-0,1
UOSVY = .060	2,5	0,0	0,0	0,0	0,003	-0,7	-1,5
UOSVY = .060	-2,2	-0,0	-0,0	-0,0	-0,003	0,7	1,5
UOSVY = .060	-5,7	-0,1	-0,0	-0,0	-0,030	2,2	10,8
UOSVZ = .060	5,2	0,1	-0,0	0,0	0,032	-2,2	-10,8
UOSVZ = .060	372,0	3,6	0,1	-0,9	-1,033	0,0	0,0
UOSVZ = .060	-371,0	-3,6	-0,1	0,9	1,034	-0,0	-0,0
SSVX = .050	-0,2	0,0	0,0	0,0	0,001	0,0	0,0
SSVY = .050	0,5	0,0	-0,0	0,0	-0,001	0,0	0,0
SSVY = .050	0,0	0,0	-0,0	0,0	0,001	0,0	0,0
SSVZ = .050	-0,5	0,0	-0,0	0,0	-0,001	0,0	0,0
SSVZ = .050	0,5	0,0	-0,0	0,0	0,001	-0,0	-0,0
SFSVX = .00003	-58,0	-1,0	-0,0	-0,5	-0,667	-0,0	-0,0
SFSVX = .00003	56,2	1,0	-4,1	0,5	0,668	0,0	0,0

~~CONFIDENTIAL~~

DIFFERENCE IN	R FT	BETA E=3 DEG	WGT LB	PHIT E=3 DEG	V FT/SEC	GINCL E=3 DEG	DNODE E=3 DEG
SFSVY = ,00003	155.2	-0.8	1.2	0.1	0.100	-0.0	-0.0
SFSVZ = ,00003	158.7	0.8	-1.2	-0.1	-0.099	0.0	0.0
ABSVY = ,00003	0.5	0.0	-0.0	0.0	0.0	0.0	0.0
ABSVZ = ,00003	-52.2	-0.8	3.2	-0.4	-0.495	-0.0	-0.0
CH11X = ,00003	51.7	0.8	-3.2	0.4	0.495	0.0	0.0
CH11Y = ,00003	-169.2	-1.2	1.1	0.1	0.177	-0.0	-0.0
CH11Z = ,00003	173.5	1.2	-1.1	-0.1	-0.178	0.0	0.0
EPSVXY = ,00003	-1.7	-0.0	-0.0	-0.0	-0.005	0.6	1.9
EPSVYZ = ,00003	2.0	0.0	0.0	0.0	0.007	-0.6	-1.9
CH12X = ,00196	2.0	0.0	-0.0	0.0	0.004	-0.5	-1.0
CH12Y = ,00196	-1.2	-0.0	-0.0	-0.0	-0.001	0.5	1.0
CH12Z = ,00573	-8.0	-0.1	-0.0	-0.0	-0.024	2.5	9.0
EPSVXX = ,00834	7.7	0.1	-0.0	0.1	0.029	-2.5	-9.0
EPSVXY = ,00834	161.7	1.2	0.4	-0.5	-0.541	0.0	0.0
EPSVYZ = ,00393	-158.0	-1.2	-0.5	0.5	0.546	0.0	0.0
CH13X = ,00196	218.5	2.9	-8.8	1.0	1.186	0.0	0.1
CH13Y = ,00834	-218.0	-2.9	8.8	-1.0	-1.184	-0.0	-0.1
CH13Z = ,00393	-0.2	0.0	0.0	0.0	0.000	0.0	0.0
EPSVXX = ,00834	0.5	0.0	-0.0	0.0	0.002	0.0	0.0
EPSVXY = ,00834	-890.2	-7.6	5.0	0.7	1.126	-0.0	-0.1
EPSVYZ = ,00278	891.2	7.6	-5.0	-0.7	-1.124	0.0	0.1
CH14X = ,00278	0.7	0.0	-0.0	0.0	0.002	0.0	0.0
CH14Y = ,00879	-0.5	0.0	-0.0	0.0	0.001	0.0	0.0
CH14Z = ,00879	12.7	0.1	-0.0	0.1	0.041	-3.8	-13.1
EPSVXX = ,00834	-11.7	-0.1	-0.0	-0.1	-0.040	3.8	13.1
EPSVXY = ,00834	9.5	-0.1	0.0	-0.1	0.014	2.3	4.6
EPSVYZ = ,00834	9.2	0.1	-0.0	0.1	0.014	-2.3	-4.6
RSS	1217.9	12.9	11.6	2.1	2.872	6.8	25.2

TABLE 6

ERRORS AT S-IVB CUTOFF DUE TO PERFORMANCE ERRORS

DIFFERENCE IN	XDOT FT/SEC	YDOT FT/SEC	ZDOT FT/SEC	X FT	Y FT	Z FT	T SEC
EDWND = 50.	4.080	12.837	0.183	-10701.7	3415.7	-127.5	0.5210
EDWND = 50.	-4.029	-12.525	-0.179	10434.6	-3391.0	124.8	-0.4993
RCRWND = 50.	0.029	0.089	0.001	-71.3	22.0	-65.3	0.0221
EDWND = 50.	0.009	0.025	0.001	-21.3	4.5	64.2	0.0193
EISP1 = 1.	5.018	-15.626	-0.211	13070.1	-4053.0	154.7	-1.7534
EISP1 = 1.	5.309	16.571	0.225	-13856.9	4291.5	-164.0	1.8275
EDWGT1 = 1.5	5.008	15.715	0.192	-13056.5	4299.0	-159.0	-2.5881
EISP2 = 1.	-4.944	-15.317	-0.218	12751.1	-4273.2	157.7	2.7918
EISP2 = 1.	8.677	27.201	0.349	-22666.3	7266.0	-278.0	-2.4909
EISP2 = 1.	-8.657	-26.904	-0.380	22435.5	-7269.2	275.1	2.5112
EDWGT2 = 3.	78.576	249.645	3.322	-203357.6	60271.7	-2589.7	15.7507
EDWGT2 = 3.	-86.250	-264.254	-3.573	220178.7	-72504.0	2651.2	-16.9741
WGT1 = 310.	0.231	0.710	0.011	-555.3	132.2	-7.1	0.0776
WGT1 = 310.	-0.230	-0.707	-0.011	594.7	-181.5	7.1	-0.0776
FUEL1 = 1.3	-1.917	-5.954	-0.076	4991.5	-1596.0	60.0	0.2139
FUEL1 = 1.3	1.933	6.041	0.077	-5040.1	1612.0	-59.0	-0.2118
FUEL2 = 1.	-19.708	-61.224	-0.629	51087.0	-16615.5	629.3	4.8272
FUEL2 = 1.	19.629	61.507	0.831	-51327.2	16577.5	-635.6	-4.7881
ETMIX = 30.	-39.939	-123.542	-1.674	10622.7	-32904.2	1278.4	6.2682
ETMIX = 30.	41.847	131.900	1.741	-110714.8	35522.2	-13369.1	-6.0711
ECD = 15.	2.215	6.989	0.075	-5844.1	1777.5	-68.9	0.7859
ECD = 15.	-2.180	-6.740	-0.107	5661.3	-1767.2	66.9	-0.7660
ECL = 15.	0.011	0.037	0.000	-29.1	11.2	-0.0	-0.0000
ECL = 15.	-0.011	-0.033	-0.000	27.6	-10.2	0.2	0.0001
ERMOA = 10.	1.224	3.924	0.062	-3283.9	1001.0	-38.5	0.4388
ERMOA = 10.	-1.231	-3.795	-0.060	3184.6	-968.0	37.4	-0.4404
RSS	98.662	304.201	4.097	254097.4	83084.1	3111.5	19.2169

TABLE 7

ERRORS AT S-IVB CUTOFF DUE TO PERFORMANCE ERRORS

	R FY	BETA E-3 DEG	WGT LB	PHIT E-3 DEG	V FY/SEC	GINCL E-3 DEG	DNODE E-3 DEG
EDWIND= 50.	-10.5	0.0	230.2	30.0	-0.028	0.0	0.0
EDWIND= 50.	-41.0	0.0	220.5	29.3	-0.012	0.0	0.0
EDWIND= 50.	-1.5	0.0	-9.8	0.2	0.000	0.2	0.1
EDWIND= 50.	-1.2	0.0	-8.5	0.1	0.001	-0.2	0.1
EISPI = 1.	134.2	0.0	774.5	36.6	-0.006	0.0	0.0
EISPI = 1.	-137.7	0.0	807.2	-38.8	0.006	0.0	0.0
EDWGT1= 1.5	112.7	0.0	199.3	36.7	-0.021	0.0	0.1
EISPI = 1.5	-172.7	0.1	-260.5	35.9	-0.030	0.0	0.1
EISPI = 1.	8.0	0.0	1100.3	63.6	-0.021	0.0	0.1
EISPI = 1.	-61.0	0.0	-1109.3	63.0	-0.020	0.0	0.1
EDWGT2= 3.	624.5	0.8	424.8	584.2	-0.007	0.2	0.0
EISPI = 3.	-488.5	0.5	531.5	620.1	-0.008	-0.1	0.0
WGT1 = 310.	-8.0	0.0	-34.3	1.7	0.003	0.0	0.0
FUEL1 = 310.	9.0	0.0	34.3	1.7	-0.004	0.0	0.0
FUEL1 = 3.	4.5	0.1	95.2	14.0	-0.009	0.0	0.0
FUEL2 = 3.	-2.5	0.0	-96.1	14.1	-0.002	0.0	0.0
FUEL2 = 1.	-162.2	0.2	154.7	143.5	-0.008	0.0	0.0
FUEL2 = 1.	187.2	0.2	-172.0	144.1	0.008	0.0	0.0
ETMIX = 30.	-504.5	0.9	17.3	290.3	-0.013	0.1	0.1
ECD = 30.	347.7	2.2	104.4	310.7	-0.021	0.1	0.1
ECD = 15.	-90.2	0.0	-347.2	16.3	-0.022	0.0	0.1
ECD = 15.	40.0	0.0	338.4	15.8	-0.019	0.0	0.1
ECL = 15.	1.7	0.0	0.0	0.1	-0.000	0.0	0.0
ECL = 15.	-1.2	0.0	-0.0	0.1	-0.000	0.0	0.0
ERMOA = 10.	-48.5	0.0	-193.8	9.2	-0.031	0.0	0.0
ERMOA = 10.	50.7	0.0	194.5	8.9	-0.014	0.0	0.0
RSS	862.9	2.4	1579.5	714.3	0.066	0.3	0.2

CONFIDENTIAL

TABLE 8
ERRORS AT 640 SEC DUE TO PLATFORM ERRORS

DIFFERENCE IN	VU FT/SEC	VV FT/SEC	VW FT/SEC	RU FT	RV FT	RW FT
GDSVX = ,100	0,010	0,004	-0,454	4,2	2,6	-268,2
GDSVY = ,100	-0,007	-0,004	0,454	-3,7	-2,9	268,3
GDSVZ = ,075	-0,044	-0,031	3,020	-9,0	-6,8	648,8
GDSVZ = ,075	0,045	0,031	-3,020	9,0	6,8	-648,8
GDSVZ = ,075	3,046	-1,460	0,022	579,2	-419,7	2,8
GDSVZ = ,075	-3,043	1,458	-0,022	-578,0	418,7	-2,7
USSVX = ,100	0,009	0,006	-0,349	3,0	2,4	-214,6
USSVY = ,100	-0,004	-0,002	0,349	-3,2	-2,1	214,5
USSVZ = ,075	-0,038	-0,026	2,442	-10,0	-6,6	648,8
USSVZ = ,075	0,039	0,026	-2,442	9,0	7,0	-648,9
USSVZ = ,100	0,002	0,000	0,000	0,0	-0,1	0,0
USSVZ = ,100	0,001	0,001	0,000	0,0	0,2	-0,1
UISVX = ,100	0,001	0,001	-0,000	0,0	0,1	0,0
UISVY = ,100	0,001	0,001	0,000	0,0	0,1	0,2
UISVY = ,075	0,001	0,002	0,001	-0,2	0,1	0,2
UISVY = ,075	0,002	0,003	-0,000	0,0	0,1	-0,1
UISVZ = ,075	3,427	-1,515	0,026	615,7	-400,5	3,6
UISVZ = ,075	-3,422	1,515	-0,026	-614,2	399,4	-3,6
UOSVX = ,060	0,008	0,002	-0,401	3,0	2,3	-223,2
UOSVY = ,060	-0,006	-0,003	0,401	-3,0	-2,3	223,2
UOSVY = ,060	-0,039	-0,027	2,709	-8,0	-5,5	540,1
UOSVY = ,060	0,040	0,029	-2,709	7,5	5,9	-540,1
UOSVZ = ,060	2,002	-1,129	0,012	451,7	-392,7	1,2
UOSVZ = ,060	-1,998	1,130	-0,012	-450,7	392,1	-1,3
SSVX = ,050	0,001	0,001	0,000	0,0	0,2	0,0
SSVY = ,050	0,002	0,001	0,000	0,7	-0,2	0,1
SSVY = ,050	0,001	0,000	0,001	0,0	0,1	0,2
SSVY = ,050	0,001	0,001	-0,000	-0,5	0,3	-0,2
SSVZ = ,050	0,002	0,001	-0,000	0,5	-0,1	0,1
SSVZ = ,050	0,001	0,001	0,000	-0,2	0,3	0,0
SFSVX = ,00003	-0,529	-0,638	-0,010	-82,2	9,0	-3,2
SFSVX = ,00003	0,529	0,639	0,011	80,2	-7,7	2,9

CONT

	DIFFERENCE IN	VU FT/SEC	VV FT/SEC	VW FT/SEC	RU FT	RV FT	RW FT
SFSVY	= ,00003	-0,495	0,121	-0,003	-172,7	128,0	-1,2
SFSVZ	= ,00003	0,504	-0,120	0,003	176,2	-131,0	1,5
ABSVX	= ,00003	0,001	0,	0,000	0,5	0,1	0,1
ABSVY	= ,00003	0,001	-0,000	-0,000	0,5	-0,1	-0,0
CH11X	= ,00196	-0,445	-0,471	-0,008	-72,7	15,5	-2,8
CH11Y	= ,00573	0,446	0,471	0,008	71,7	-14,9	2,8
CH11Z	= ,00196	-0,705	0,211	-0,005	-197,5	132,7	-1,6
EPSVXY	= ,00834	0,716	-0,211	0,005	201,5	-136,3	1,7
EPSVYZ	= ,00393	-0,007	-0,004	0,496	-2,5	-2,0	184,4
CH11X	= ,00196	0,009	0,006	-0,496	2,5	2,1	-184,4
CH11Y	= ,00573	0,007	0,003	-0,283	2,2	1,6	-173,7
CH11Z	= ,00196	-0,004	-0,001	0,283	-1,7	2,2	173,6
EPSVXY	= ,00834	-0,036	-0,022	2,303	-10,2	-7,2	703,3
EPSVYZ	= ,00393	0,038	0,027	-2,302	9,7	7,6	-703,5
CH11X	= ,00196	0,751	-0,572	0,003	188,0	-214,6	-0,3
CH11Y	= ,00573	-0,739	0,577	-0,003	-184,0	211,3	0,5
CH11Z	= ,00196	1,562	1,104	0,019	287,0	-105,5	11,0
EPSVXY	= ,00834	-1,558	-1,102	-0,019	-286,5	105,5	-11,0
EPSVYZ	= ,00393	0,000	0,000	0,000	-0,2	0,3	0,0
CH11X	= ,00196	0,002	0,002	0,000	0,5	-0,0	0,1
CH11Y	= ,00573	-4,156	1,331	-0,029	-1060,7	685,9	-8,9
CH11Z	= ,00196	4,162	-1,329	0,029	1061,7	-687,2	9,0
EPSVXY	= ,00834	0,001	0,002	0,000	0,7	-0,1	-0,0
EPSVYZ	= ,00248	0,001	0,001	0,000	-0,2	0,4	0,0
CH11X	= ,00196	0,056	0,037	-3,341	16,0	10,8	-1052,8
CH11Y	= ,00573	-0,054	-0,037	3,341	-15,0	-11,4	1052,9
CH11Z	= ,00196	-0,024	-0,012	1,226	-11,5	-7,4	740,7
EPSVXY	= ,00834	0,026	0,012	-1,226	10,7	7,4	-740,5
RSS		6,828	3,117	6,419	1499,4	1027,9	1875,6

TABLE 9

ERRORS AT 640 SEC DUE TO PERFORMANCE ERRORS

DIFFERENCE IN	VU FT/SEC	VV FT/SEC	VM FT/SEC	RU FT	RV FT	RW FT
HEDWND= 50,	29,424	-0,048	0,011	-29,5	-24627,3	-3,4
"50,	-28,453	-0,024	-0,011	-50,2	23806,2	2,2
RCRWND= 50,	0,770	0,	-0,004	-1,7	-643,3	64,1
"50,	0,617	0,001	0,005	-1,5	-516,9	-64,3
EISPI = 1,	-70,087	-0,101	-0,074	69,5	58742,1	5,4
"1,	73,346	-0,101	0,075	-241,7	-61468,0	-6,1
EDWGT1= 1,5	-62,746	-0,115	-0,092	73,0	52765,3	2,0
"1,5	69,372	-0,109	0,131	-276,0	-58297,4	-3,6
EISPI2 = 1,	-47,727	-0,086	-0,089	-7,2	40195,8	3,0
"1,	48,627	-0,046	0,125	-122,2	-40954,5	-2,0
EDWGT2= 3,	-220,488	-1,116	-0,660	-40,7	186122,2	46,2
"3,	241,770	-1,014	0,718	-1579,0	-204131,8	-31,2
WGT1 = 310,	3,122	0,003	0,002	-9,0	-2616,3	-0,4
"310,	-3,117	0,004	0,002	9,2	2614,3	0,4
FUEL1 = 3	0,297	-0,007	0,005	4,0	-258,6	0,0
"3	-0,144	-0,005	-0,004	-0,7	152,0	-1,3
FUEL2 = 1,	83,484	-0,107	0,210	-315,7	-70335,7	-10,4
"1,	-82,031	-0,163	-0,209	116,2	69111,6	11,8
ETMIX = 30,	62,046	-0,037	0,276	-605,0	-52427,1	-30,4
"30,	-47,481	-0,080	-0,233	313,2	39737,2	23,4
ECD = 15,	31,384	-0,042	0,052	-113,0	-26303,6	-2,0
"15,	-30,537	-0,037	-0,017	31,7	25596,9	2,9
ECL = 15,	0,038	-0,000	0,000	1,7	-30,6	-0,2
"15,	-0,032	-0,000	-0,000	-1,2	26,9	0,2
ERMOA = 10,	17,538	-0,037	0,009	-58,2	-14708,7	-2,2
"10,	-17,469	-0,020	-0,010	49,7	14643,6	2,3
RSS	289,823	1,146	0,823	1768,4	244421,2	86,1

TABLE 10
ERRORS AT 640 SEC DUE TO PLATFORM ERRORS

DIFFERENCE IN	VNU FT/SEC	VNV FT/SEC	VNW FT/SEC	RNU FT	RNV FT	RNW FT
GDSVX = ,100	0,001	0,000	0,000	0,2	0,1	0,2
GDSVX = ,100	0,001	0,001	0,000	0,2	0,3	0,5
GDSVY = ,075	0,001	0,001	0,001	0,2	0,1	0,5
GDSVZ = ,075	0,000	0,001	0,001	0,2	0,1	0,3
GDSVZ = ,075	0,016	0,001	0,000	0,2	12,8	0,3
GDSVZ = ,075	0,019	0,001	0,000	0,2	14,2	0,1
USSVX = ,100	0,001	0,002	0,001	0,1	0,4	0,1
USSVX = ,100	0,001	0,000	0,001	0,1	0,3	0,2
USSVY = ,075	0,001	0,001	0,000	0,1	0,2	0,6
USSVZ = ,075	0,001	0,001	0,000	0,1	0,5	0,4
USSVZ = ,100	0,001	0,002	0,000	0,2	0,1	0,1
UISVX = ,100	0,001	0,001	0,000	0,2	0,3	0,1
UISVX = ,100	0,001	0,001	0,000	0,2	0,1	0,1
UISVY = ,075	0,001	0,000	0,000	0,1	0,2	0,1
UISVY = ,075	0,001	0,002	0,000	0,1	0,3	0,1
UISVZ = ,075	0,001	0,002	0,000	0,1	0,2	0,1
UISVZ = ,075	0,006	0,002	0,000	0,5	3,1	0,0
UISVZ = ,075	0,009	0,002	0,000	0,7	4,6	0,1
UOSVX = ,060	0,000	0,002	0,000	0,5	0,2	0,4
UOSVX = ,060	0,001	0,001	0,000	0,2	0,4	0,5
UOSVY = ,060	0,001	0,003	0,002	0,1	0,2	0,6
UOSVY = ,060	0,001	0,001	0,002	0,1	0,2	0,4
UOSVZ = ,060	0,017	0,000	0,000	0,1	14,5	0,0
UOSVZ = ,060	0,019	0,002	0,000	0,5	15,7	0,1
SSVX = ,050	0,000	0,001	0,000	0,2	0,1	0,1
SSVX = ,050	0,001	0,001	0,000	0,1	0,3	0,1
SSVY = ,050	0,001	0,001	0,000	0,1	0,2	0,1
SSVY = ,050	0,001	0,002	0,000	0,1	0,2	0,1
SSVZ = ,050	0,000	0,000	0,000	0,1	0,2	0,1
SSVZ = ,050	0,001	0,002	0,000	0,1	0,1	0,1
SFSVX = ,00003	0,237	0,001	0,000	0,2	203,7	0,1
SFSVX = ,00003	0,239	0,001	0,000	1,0	204,0	0,1

CONFIDENTIAL

DIFFERENCE IN	VNU FT/SEC	VNV FT/SEC	VNH FT/SEC	RNU FT	RNV FT	RNW FT
SFSVY = ,00003	-0,081	0,	-0,000	0,2	64,7	-0,1
SFSVZ = ,00003	0,085	0,001	0,000	0,	-67,7	-0,1
SFSVZ = ,00003	0,000	0,000	-0,000	0,	-0,1	-0,1
SFSVZ = ,00003	0,001	-0,000	0,000	0,	-0,2	-0,1
ABSVX = ,00003	-0,203	0,046	0,001	2,2	188,6	-0,0
ABSVX = ,00003	0,206	-0,045	-0,001	-2,0	-189,6	0,0
ABSVY = ,00003	-0,010	-0,018	0,001	4,2	58,4	-0,1
ABSVY = ,00003	0,013	0,019	-0,000	-4,0	-61,4	0,0
ABSVZ = ,00003	0,002	0,002	-0,063	0,2	-0,2	-4,0
ABSVZ = ,00003	-0,000	0,001	0,063	-0,5	-0,1	3,8
CH1X = ,00196	0,001	0,001	0,000	-0,2	-0,6	0,2
CH1X = ,00196	0,001	0,001	0,000	-0,2	-0,3	-0,4
CH1Y = ,00573	0,001	0,001	0,000	0,	-0,3	-0,8
CH1Y = ,00573	0,001	0,002	0,000	0,	-0,1	0,5
CH1Z = ,00196	-0,048	0,002	0,000	-0,7	40,5	-0,1
CH1Z = ,00196	0,053	0,002	0,000	0,2	-43,7	-0,2
EPSVXY = ,00834	0,951	0,001	0,001	-0,5	-792,9	-0,0
EPSVXY = ,00834	-0,948	-0,000	-0,000	0,	791,2	-0,1
EPSVXZ = ,00393	0,000	0,001	0,000	0,	0,	0,
EPSVXZ = ,00393	0,001	0,002	0,000	0,	-0,4	0,
EPSVYX = ,00834	-0,153	-0,010	0,002	25,7	284,9	0,1
EPSVYX = ,00834	0,156	0,012	-0,002	-25,7	-287,0	-0,5
GPSVYZ = ,00248	0,001	0,002	-0,000	0,	0,	0,
GPSVYZ = ,00278	0,001	0,001	0,000	-0,2	-0,1	-0,1
EPSVZX = ,00871	-0,001	0,001	0,191	-0,5	-0,8	27,1
EPSVZX = ,00879	0,002	0,001	-0,191	0,2	0,2	-27,3
EPSVZY = ,00834	0,000	0,001	0,022	-0,2	0,0	0,3
EPSVZY = ,00834	0,002	0,000	-0,022	0,	-0,8	-0,4
RSS	1,019	0,052	0,203	26,3	894,1	27,7

TABLE 11

ERRORS AT 640 SEC DUE TO PERFORMANCE ERRORS

DIFFERENCE IN	VNU FT/SEC	VNV FT/SEC	VNW FT/SEC	RNU FT	RNV FT	RNW FT
HEDWND= 50.	29,421	-0,048	0,012	-31,5	-24626,5	-3,5
"50.	-28,457	-0,023	-0,011	-56,0	23807,3	2,0
RCRWND= 50.	0,769	0,001	-0,004	-3,0	-643,3	64,2
"50.	0,617	0,001	0,005	-1,5	-517,6	64,6
EISPI = 1.	-70,090	-0,100	-0,074	68,7	58741,6	5,4
"1.	73,345	-0,100	0,076	-241,7	-61468,0	-6,1
EDWGT1= 1,5	-62,747	-0,115	-0,092	73,2	52768,3	2,0
"1,5	69,349	-0,091	0,131	-301,7	-58306,6	-4,1
EISPI2 = 1.	-47,727	-0,086	-0,090	-6,5	40195,1	2,8
"1.	48,628	-0,045	0,125	-120,7	-40955,5	-2,4
EDWGT2= 3.	-220,486	-1,116	-0,660	-38,5	186121,7	46,3
"3.	241,772	-1,010	0,719	-1577,2	-204132,3	-31,3
WGT1 = 310.	3,122	0,004	0,002	-9,2	-2616,1	-0,6
"310.	-3,119	-0,001	-0,002	7,7	2614,4	0,1
FUEL1 = .3	0,274	0,010	0,005	-20,5	-267,2	-0,4
"3	-0,141	-0,008	-0,004	2,7	155,0	-1,3
FUEL2 = 1.	83,480	-0,104	0,210	-320,2	-70334,0	-10,5
"1.	-82,032	-0,162	-0,209	116,0	69111,5	11,8
ETMIX = 30.	62,046	-0,037	0,276	-605,2	-52426,5	-30,4
"30.	-47,480	-0,080	-0,233	315,0	39739,5	23,3
ECD = 15.	31,383	-0,042	0,052	-114,7	-26302,6	-2,0
"15.	-30,539	-0,035	-0,017	31,2	25596,6	2,8
ECL = 15.	0,037	0,002	0,000	-0,5	-30,0	-0,3
"15.	-0,031	0,002	-0,000	-0,7	26,6	0,1
ERHOA = 10.	17,535	-0,035	0,009	-60,2	-14707,9	-2,3
"10.	-17,470	-0,017	-0,010	48,7	14644,3	2,3
RSS	289,818	1,146	0,823	1772,3	244423,2	86,4

VI. Analytical Investigations

The purpose of this section is to determine analytically the performance of certain system functions which operate in the presence of noise. The specific areas studied are:

- (1) Noise and dynamic response of the M/F filter.
- (2) Noise response of the Navigation equations (Average G Equations).
- (3) The effect of noise on the prediction of the cutoff time.

The noise source considered is the quantization in the accelerometer registers. A model for this noise source is developed.

A. Noise Model

At a set of discrete time instants, $\{t_j\}$ $j = 0, 1, \dots, n$, velocity measurements $V_i(t_j)$ $i = 1, 2, 3$ are made by three integrating accelerometers mounted orthogonally on an inertial platform

$$\bar{V}_a(t_j) = \int_0^{t_j} a_T(t) \mathcal{I}(t) dt + \bar{\delta}(t_j) \quad (1)$$

Here

$$(a) \quad \bar{V}_a(t_j) = \begin{bmatrix} V_1(t_j) \\ V_2(t_j) \\ V_3(t_j) \end{bmatrix} \quad (2)$$

represents the vector of accelerometer readings.

(b) $a_T(t)$ represents the magnitude of the thrust acceleration.

(c) $\bar{L}(t)$ is the direction cosine vector of the thrust acceleration vector in platform coordinates.

(d) $\bar{\delta}(t)$ represents the vector of errors introduced by quantization.

For the purpose of this analysis it will be assumed that the thrust acceleration is such as to cause the velocities in all three platform coordinates to be monotonically increasing functions of time. With this assumption together with zero initial velocity stored in the accelerometers, the accelerometer readings will be lower than the true values. Each component of the quantization noise thus has the probability density function

$$p(\delta_i(t_j)) = \begin{cases} \frac{1}{b} & -b < \delta_i(t_j) < 0 \\ 0 & \text{elsewhere} \end{cases} \quad (3)$$

where $b = .164$ ft/sec (.05 meters/sec) is the value of the least significant bit in each accelerometer register.

Thus the mean of the quantization noise is

$$E\{\delta_i(t)\} = -\frac{b}{2} \text{ ft/sec} = -.082 \text{ ft/sec} \quad (4)$$

and the variance about the mean is

$$E\left\{\left(\delta_i(t) + \frac{b}{2}\right)^2\right\} = \frac{b^2}{12} \text{ ft}^2/\text{sec}^2 = .00224 \text{ ft}^2/\text{sec}^2 \quad (5)$$

The noise is also assumed to be uncorrelated, i.e.,

$$E\left\{\left(\delta_i(t_j) + \frac{b}{2}\right)\left(\delta_i(t_k) + \frac{b}{2}\right)\right\} = 0 \quad \text{for } j \neq k.$$

The above model has assumed zero initial conditions for the accelerometers. However, since the accelerometers are running before launch, the initial conditions are actually random variables which are uniformly distributed over the quantum interval. The effects of these initial conditions are included in the analysis.

B. Noise and Dynamic Response of the M/F Filter

The change in velocity over a one cycle interval can be obtained from (1).

~~CONFIDENTIAL~~

$$\bar{V}_a(t_j) - \bar{V}_a(t_{j-1}) = \Delta \bar{V}_a(t_j) = \int_{t_{j-1}}^{t_j} a_T(t) \mathcal{I}(t) dt + \bar{\delta}(t_j) - \bar{\delta}(t_{j-1})$$

$$\Delta \bar{V}_a(t_j) = \Delta \bar{V}(t_j) + \Delta \bar{\delta}(t_j) \quad (6)$$

Here $\Delta \bar{V}_a$ represents the measured change in velocity and $\Delta \bar{V}(t_j)$ represents the actual change in velocity.

A raw estimate (F/M) of thrust acceleration can be formed by

$$(F/M)_j = \frac{\| \Delta \bar{V}_a(t_j) \|}{\Delta T} \quad (7)$$

where $\| \bar{x} \|$ represents the Euclidean norm $\left(\sum_{i=1}^3 x_i^2 \right)^{1/2}$ of the enclosed three dimensional vector and $\Delta T = t_j - t_{j-1}$ is nominally 1.7 seconds.

In the absence of noise F/M closely approximates the true value of thrust acceleration which is inversely proportional to a linear function of time.

In order to obtain an estimate of a_T , a filter has been designed⁸ which operates on the (M/F) data points, which nominally lie on a straight line $\left(M/F \approx \frac{1}{a_T} \right)$ which is linear).

The filter specification is obtained by digitalizing the following transfer function

$$\frac{(M/F)^S}{(M/F)} = \frac{1 + 42s}{1 + 42s + 520s^2 + 1848s^3 + 1936s^4} \quad (3)$$

When this transfer function is put into the form of a negative feedback system, the resulting system is seen to be of type 2. Thus the continuous filter will follow a ramp input (which is the expected input) with no steady state error.

The transfer function given by (8) is digitalized⁸ to yield the following difference equation:

$$\begin{aligned} (M/F)_i^S = & 2.8048253(M/F)_{i-1}^S - 2.8588037(M/F)_{i-2}^S \\ & + 1.2493337(M/F)_{i-3}^S - 0.19735971(M/F)_{i-4}^S \\ & + 0.012095511(M/F)_i + 0.021333516(M/F)_{i-1} \\ & - 0.026158031(M/F)_{i-2} - 0.0052666918(M/F)_{i-3} \end{aligned} \quad (9)$$

The discrete time filter has a steady state error for a ramp input. This error corresponds to a time lead of .85 seconds which is $\Delta T/2$. If it is assumed that $(F/M)_j$ computed from (7) is valid at $t_{j-1} + \frac{\Delta T}{2}$, the total time delay is zero, thereby providing an unbiased estimate.

In order to obtain the noise response of the filter it is necessary to solve the difference equation (9). Solution of this equation results in the filter weighting sequence which can be used to obtain the output noise variance.

Equation (9) may be transformed into the z domain to yield the following transfer function

$$H(z) = \frac{N(z)}{D(z)}$$

$$N(z) = 0.012095511z^4 + 0.021333516z^3 \\ - 0.026158031z^2 - 0.0052666918z$$

$$D(z) = (z-z_1)(z-z_2)(z-z_3)(z-z_4)$$

where

$$z_1 = 0.55836431$$

$$z_2 = 0.89341121$$

$$z_3 = 0.92563474$$

$$z_4 = 0.42741504$$

Inverting $H(z)$ yields the weighting sequence valid for $k > 0$

$$h(k) = - 0.3851741(z_1)^{k-1} + 0.5297386(z_2)^{k-1} \\ - 0.25246(z_3)^{k-1} + 0.1631549(z_4)^{k-1} \quad (10)$$

and

$$h(0) = 0.012095511$$

Figure 8 shows a plot of this function and Figure 9 shows the unit step response which is given by

$$(M/F)_n^s = \sum_{i=0}^n h(i)$$

For an input which consists of uncorrelated, zero mean, stationary noise samples of variance σ_{in}^2 , the standard deviation of the output noise is given by

$$\sigma_{out}(k) = \left[\sum_{i=0}^k h^2(i) \right]^{1/2} \sigma_{in}$$

It is seen from Figure 10 that σ_{out} settles to .323 σ_{in} resulting in a 67.7% noise reduction.

C. Noise Response of the Powered Flight Navigation Equations ("Average G Equations")

It has been shown⁹ that the Saturn navigation equations can be expressed by

$$\bar{R}_n = \bar{R}_{n-1} + \bar{V}_{n-1} \Delta T + \frac{1}{2} [\Delta \bar{V}_a(n) + \bar{G}_{n-1} \Delta T] \Delta T \quad (11a)$$

$$\bar{G}_n = \bar{G}(\bar{R}_n)$$

$$\bar{V}_n = \bar{V}_{n-1} + \Delta \bar{V}_a(n) + \frac{1}{2} [\bar{G}_n + \bar{G}_{n-1}] \Delta T \quad (11b)$$

where

- a) $\Delta \bar{V}_a$ is the change in velocity, due to thrust acceleration, as measured by the accelerometers.
- b) \bar{R}_n is the estimate of the position vector at time t_n .
- c) \bar{V}_n is the estimate of the velocity vector at time t_n .
- d) \bar{G}_n is the gravitational acceleration vector which is a non-linear function of \bar{R}_n .
- e) ΔT is the computation cycle time.

In a recent paper¹⁵ the effect of noise in ΔV_a on the output of these equations was analytically determined. The one dimensional problem was considered and the model used for gravity was

$$G_n = - \mu / R_n^2 \quad (11c)$$

Equations (11) represent a set of non-linear, coupled, difference equations for the navigation position and velocity (the non-linearity being due to the gravity term). In order to determine the statistics of the errors resulting from noisy measurements (ΔV_a) the gravity equation

(11c) was linearized about a nominal value. The position equation (11a) was then uncoupled from (11b) in such a way as to yield a second order difference equation for the noise in position. The solution of this equation yielded a weighting sequence (impulse response) which was used to determine the statistics of the resulting position errors. The weighting sequence was then used to determine the statistics of the navigation velocity errors introduced by the coupling through the gravity terms.

In this section the results derived in Reference 15 will be applied to an error analysis of the Saturn launch vehicle navigation equations. The error source considered here is quantization in the accelerometer registers. A model for quantization has been formed in Reference 14 and the resulting statistics are

$$E\{\delta V_a\} = - .082 \text{ ft./sec.}$$

and

$$E\{(\delta V_a + .082)^2\} = \sigma_a^2 = 0.0474 \text{ ft./sec.}^2$$

The results quoted here will be for $n = 353$ and $\Delta T = 1.7$ seconds ($n\Delta T \approx 600$ seconds).

By using the equations derived in Reference 15 including the effects of initial conditions, the mean of the position error is found to be

$$E\{\delta R_{353}\} = 0. \text{ ft.}$$

and the standard deviation about this mean is

$$\sigma_{\delta R_{353}} = 34. \text{ ft.}$$

The mean of the velocity error is found to be

$$E\{\delta V_{353}\} = 0. \text{ ft./sec.}$$

and the standard deviation about this mean is

$$\sigma_{\delta V_{353}} = 0.047 (\sqrt{2}) = 0.066 \text{ ft./sec.}$$

Here the standard deviation of the velocity error is due to the noise in the most recent accelerometer measurement and the random initial conditions.

The conclusion of this analysis is that the output of the position navigation equation is unbiased and has a standard deviation of 34. feet. The output of the velocity navigation equation is also unbiased and has a standard deviation of 0.066 ft./sec.

D. The Effect of Noise on the Prediction of the
Cutoff Time

In this section the scheme used to determine the cutoff time* of the S-IVB will be evaluated.

The procedure used is to fit a second degree polynomial to the magnitude of the three most recent velocities obtained from the navigation equations. The velocity data is then extrapolated, using the polynomial, to determine the time at which the predicted velocity would equal the desired terminal velocity (V_T).

Let V_2 , V_1 , V_0 be the three most recent velocities obtained from the navigation equations at times t_2 , t_1 , and t_0 respectively, where

$$t_2 > t_1 > t_0$$

$$t_2 - t_1 = \Delta t_2, \quad t_1 - t_0 = \Delta t_1$$

and

$$t_2 - t_0 = \Delta t_3$$

* It is assumed that the scheme used is that outlined in the LVDC Equation Defining Document for the AS-204 Flight Program.⁵

The resulting extrapolating polynomial is

$$a_2 t_g^2 + a_1 t_g + V_2 - V_T = 0 \quad (12)$$

where t_g is the predicted time to go required to achieve V_T .

The coefficients of the polynomial are

$$a_2 = \frac{(V_2 - V_1)\Delta t_1 - (V_1 - V_0)\Delta t_2}{\Delta t_2 \Delta t_1 \Delta t_3}$$

$$a_1 = \frac{V_2 - V_1}{\Delta t_2} + a_2 \Delta t_2$$

The method proposed to solve (12) for t_g is recursive

$$t_g = \frac{V_T - V_2}{a_1 + a_2 t_g}$$

where the t_g appearing in the denominator is the previous estimate minus Δt_2 , i.e.,

$$(t_g)_{t_2} = \frac{V_T - V_2}{a_1 + a_2 \left[(t_g)_{t_1} - \Delta t_2 \right]} \quad (13)$$

Since a_2 is small the quadratic is not solved directly. For the purpose of the noise analysis of the cut-off scheme it will be assumed that (13) is an exact solution of (12).

Let the velocity output of the navigation equations be represented by

$$V(t) = P(t) + n(t) + \delta V_0 \quad (14)$$

where

- (a) $P(t)$ represents the actual velocity assumed to be a second degree polynomial in time.
- (b) $n(t)$ is the noise output of the navigation equations due to quantization. The one sigma value of $n(t)$ is .0474 ft/sec. It should also be remembered that $n(t)$ is an uncorrelated process.
- (c) δV_0 represents the initial conditions of the accelerometers at liftoff. The one sigma value of δV_0 is also .0474 ft/sec.

Since δV_0 is a constant during the flight, it affects all computations of V and thus affects the terminal velocity directly. However, since $n(t)$ is an uncorrelated process, the standard deviation of the error in terminal velocity (σ_0) due to $n(t)$ is a function of the number of prediction cycles and the level of the input noise ($\sigma_1(t)$) as shown in Figure 11.

For the problem under consideration,

$$\sigma_i = .0474 \text{ ft/sec.}$$

and M , which is the number of points used in the fit, is 3. The cutoff calculation is terminated when the prediction time is between 0.8 and 1.8 cycles, and the current estimate of t_g is used to command cutoff.

The prediction time (t_p) is now treated as a random variable uniformly distributed from 0.8 cycles to 1.8 cycles. The density function for t_p is

$$p(t_p) = \begin{cases} \frac{1}{\Delta T} & 0.8\Delta T < t_p < 1.8\Delta T \\ 0 & \text{elsewhere} \end{cases}$$

It can be shown that the conditional variance of the velocity error at cutoff (t_{co}) given the prediction time is given by

$$\begin{aligned} & E \left\{ \left[P(t_{co}) - V_T \right]^2 / t_p \right\} \\ &= \sigma_i^2 \left[1 + \frac{3t_p}{\Delta T} + \frac{15}{2} \left(\frac{t_p}{\Delta T} \right)^2 + 6 \left(\frac{t_p}{\Delta T} \right)^3 + \frac{3}{2} \left(\frac{t_p}{\Delta T} \right)^4 \right] \end{aligned}$$

Now the variance of the velocity error at cutoff is given by

$$\sigma_0^2 = E \left\{ \left[P(t_{co}) - V_T \right]^2 \right\} = \int_{-\infty}^{\infty} E \left\{ \left[P(t_{co}) - V_T \right]^2 / t_p \right\} p(t_p) dt_p.$$

Letting $x = \frac{t_p}{\Delta T}$ yields

$$\frac{\sigma_0^2}{\sigma_1^2} = \int_{0.8}^{1.8} \left(1 + 3x + \frac{15}{2} x^2 + 6x^3 + \frac{3}{2} x^4 \right) dx = 38.9$$

or

$$\frac{\sigma_0}{\sigma_1} = 6.23.$$

Thus the standard deviation of the error in cutoff velocity due to quantization in the measurements during the flight and initial velocity stored in the accelerometers at liftoff is

$$\sigma = (.0474) \left\{ (6.23)^2 + (1)^2 \right\}^{\frac{1}{2}} = .299 \text{ ft/sec.}$$

The three sigma deviation of .897 ft/sec. has been included in the velocity magnitude uncertainty listed on page 17.

REFERENCES

1. AS-204 Launch Vehicle Operational Flight Trajectory, CCSD TN-AP-66-70, Sept. 14, 1966.
2. Bellcomm Apollo Simulation Program Operations Manual, 7094 IBSYS Procedures, Jan. 1, 1965.
3. Bellcomm Apollo Simulation Program Maintenance Manual, 7094 IBSYS Procedures, Jan. 1, 1965.
4. Amman, R. J.: Bellcomm Apollo Simulation Program Revisions - October 11, 1965 - Delivery to Bellcomm, BTL MF5-4264-34, Oct. 8, 1965.
5. LVDC Equation Defining Document - AS-204, IBM 65-207-0009H, Nov. 15, 1965.
6. Smith, O. E. and Weidner, Don K.: A Reference Atmosphere for Patrick AFB, Florida, Annual (1963 Revision), NASA TM X-53139, Sept. 23, 1964.
7. Natural Environment and Physical Standards for the Apollo Program, NASA SE-015-001-1, April 1965.
8. Hosenthien, H. H.: AS-204 M/F Filter, MSFC R-ASTR-F-66-139.
9. Bamesberger, G.: Comparison of MIT and MSFC Near Earth Navigation Schemes, BTL MF6-4264-5, Feb. 10, 1966.
10. ST-124M Platform Hardware Errors, MSFC R-ASTR-NG-109-66, Confidential, July 22, 1966.
11. AS-204 Launch Vehicle Operational Flight Trajectory Dispersion Analysis, CCSD TN-AP-66-72, Sept. 26, 1966.
12. 3-Sigma Mass Deviations Based on the 1964 Saturn I Flights, MSFC Issue No. 9, Jan. 15, 1966.
13. McDaniel, Gary: The First Stage Optimization of the Saturn V Vehicle, NASA TM X-53225, March 25, 1965.
14. Launch Vehicle Error Analysis of Apollo/Saturn 202 (U), Confidential, BTL, July 15, 1966.
15. Heffes, H.: Noise Analysis of the Apollo Powered Flight Navigation Equations, BTL MM66-4264-13, Aug. 31, 1966.

APPENDIX

Definition of Coordinate Systems

Platform Coordinates

The platform coordinate system (x,y,z) is an earth centered inertial system defined with the y-axis upward along the local vertical at launch, the x-axis perpendicular to the y-axis, pointing downrange along the launch azimuth, and the z-axis completing a right handed orthogonal coordinate system.

UVW Coordinates

The UVW coordinate system is an earth centered inertial system defined relative to the state vector at 640 sec on the nominal closed loop reference trajectory. U is defined as upward along the position vector, V is along the projection of the velocity vector in a plane perpendicular to U, and W completes the right handed orthogonal system.

DEFINITION OF SYMBOLS

Observed Trajectory Variables

<u>Symbol</u>	<u>Units</u>	<u>Description</u>
XDOT	ft/sec	{ velocity in platform coordinates
YDOT	ft/sec	
ZDOT	ft/sec	

<u>Symbol</u>	<u>Units</u>	<u>Description</u>
X	ft	{ position in platform coordinates
Y	ft	
Z	ft	
V	ft/sec	magnitude of velocity vector
R	ft	magnitude of position vector
T	sec	time from launch
BETAI	deg	inertial flight path angle
WGT	lbm	mass of vehicle
PHIT	deg	central angle flown by vehicle
GINCL	deg	inclination of orbit
DNODE	deg	angle from launch meridian to descending node
VU	ft/sec	{ velocity in UVW coordinates
VV	ft/sec	
VW	ft/sec	
RU	ft	{ position in UVW coordinates
RV	ft	
RW	ft	
VNU	ft/sec	{ navigation estimate of velocity in UVW coordinates
VNV	ft/sec	
VNW	ft/sec	
RNU	ft	{ navigation estimate of position in UVW coordinates
RNV	ft	
RNW	ft	

Platform Errors

<u>Symbol</u>	<u>Units</u>	<u>Description</u>
GDSVX	deg/hr	{ steady state gyro drift rates about X, Y, and Z axes
GDSVY	deg/hr	
GDSVZ	deg/hr	
USSVX	deg/hr/g	{ gyro drift due to mass unbalance about spin axis
USSVY	deg/hr/g	
USSVZ	deg/hr/g	
UISVX	deg/hr/g	{ gyro drift due to mass unbalance about input axis
UISVY	deg/hr/g	
UISVZ	deg/hr/g	
UOSVX	deg/hr/g	{ gyro drift due to mass unbalance about output axis
UOSVY	deg/hr/g	
UOSVZ	deg/hr/g	
SSVX	deg/hr/g ²	{ gyro drift due to anisoelastic effects
SSVY	deg/hr/g ²	
SSVZ	deg/hr/g ²	
SFSVX	-	{ accelerometer scale factors
SFSVY	-	
SFSVZ	-	
ABSVX	g	{ accelerometer bias
ABSVY	g	
ABSVZ	g	

<u>Symbol</u>	<u>Units</u>	<u>Description</u>
CHI1X	deg	{ initial platform misalignment
CHI1Y	deg	
CHI1Z	deg	
EPSVXY	deg	{ accelerometer misalignment co-
EPSVXZ	deg	
EPSVYX	deg	
EPSVYZ	deg	
EPSVZX	deg	
EPSVZY	deg	

Performance Errors

<u>Symbol</u>	<u>Units</u>	<u>Description</u>
HEDWND	ft/sec	horizontal wind in pitch plane, opposing vehicle's motion
RCRWND	ft/sec	horizontal wind from right side along pitch axis
EISP1	%	error in first stage specific im- pulse, weight rate held constant
EDWGT1	%	error in first stage weight rate, specific impulse held constant
EISP2	%	error in second stage specific im- pulse, weight rate held constant

<u>Symbol</u>	<u>Units</u>	<u>Description</u>
EDWGT2	%	error in second stage weight rate, specific impulse held constant
WGT1	lbm	error in first stage dry mass
EFUEL1	%	error in first stage fuel loading
EFUEL2	%	error in second stage fuel loading
ETMIX2	sec	error in time of mixture ratio shift
ECD	%	error in drag coefficient
ECL	%	error in lift coefficient
ERHOA	%	error in atmosphere's density

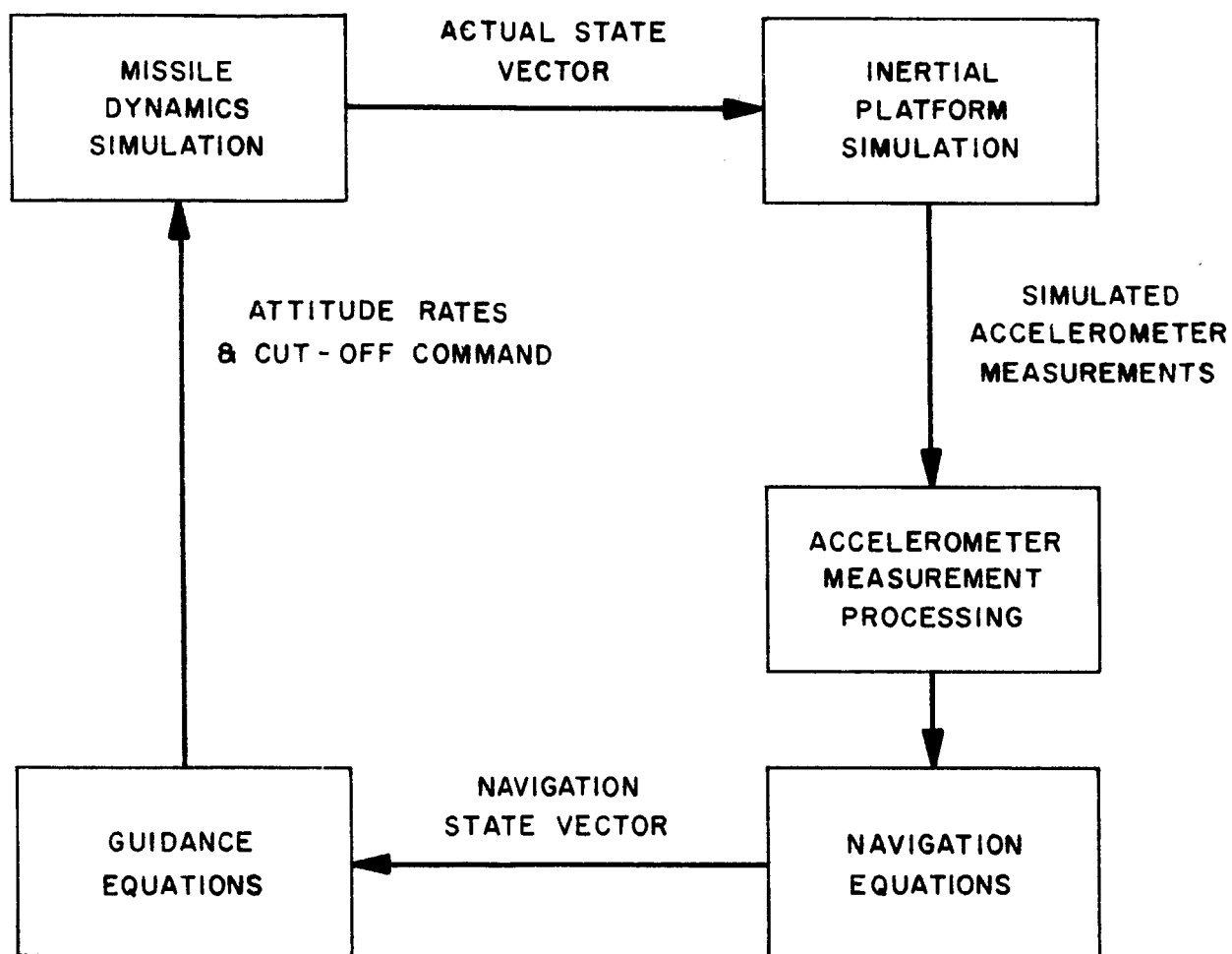


FIGURE 1
CLOSED LOOP SIMULATION

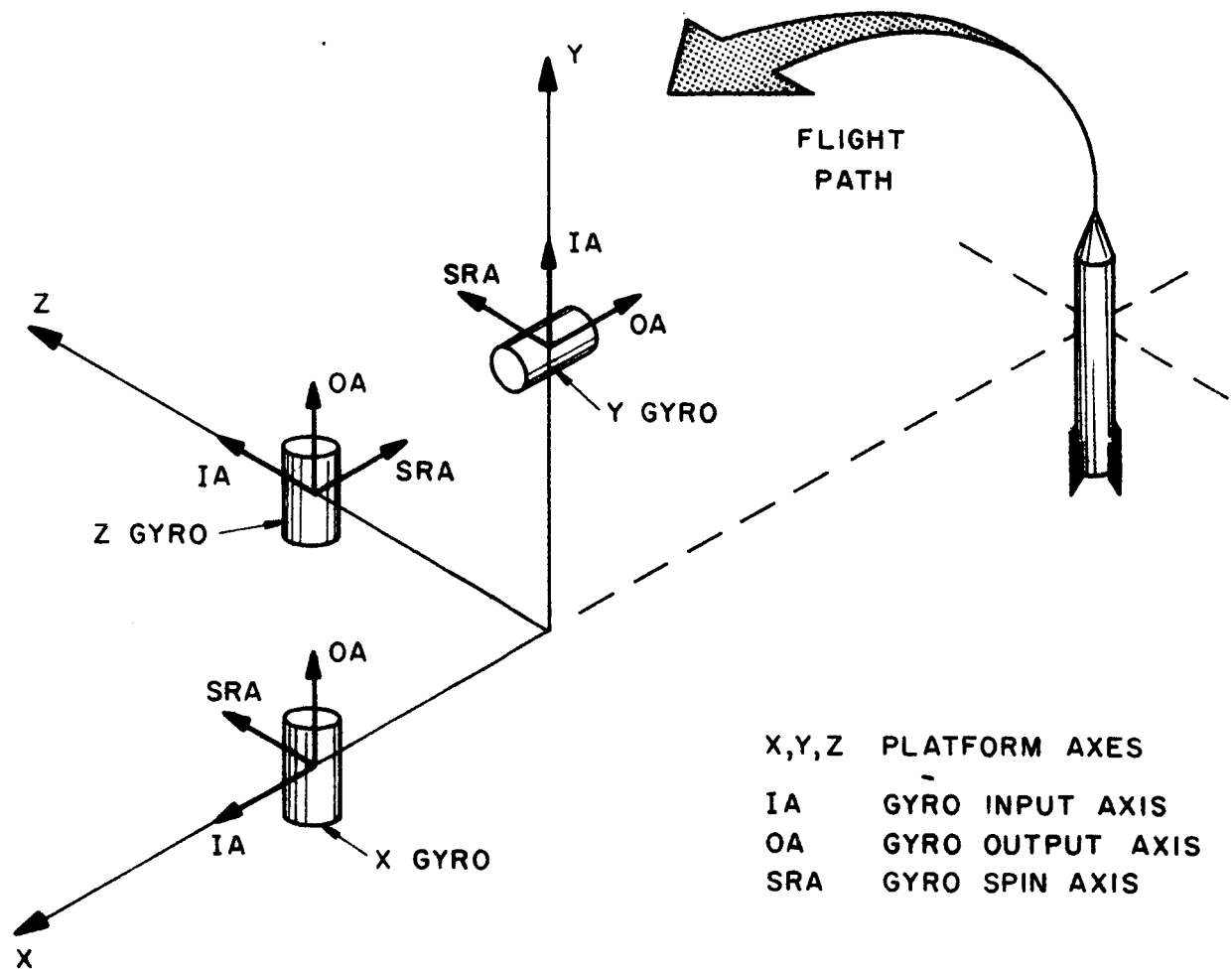


FIGURE 2
PLATFORM CONFIGURATION

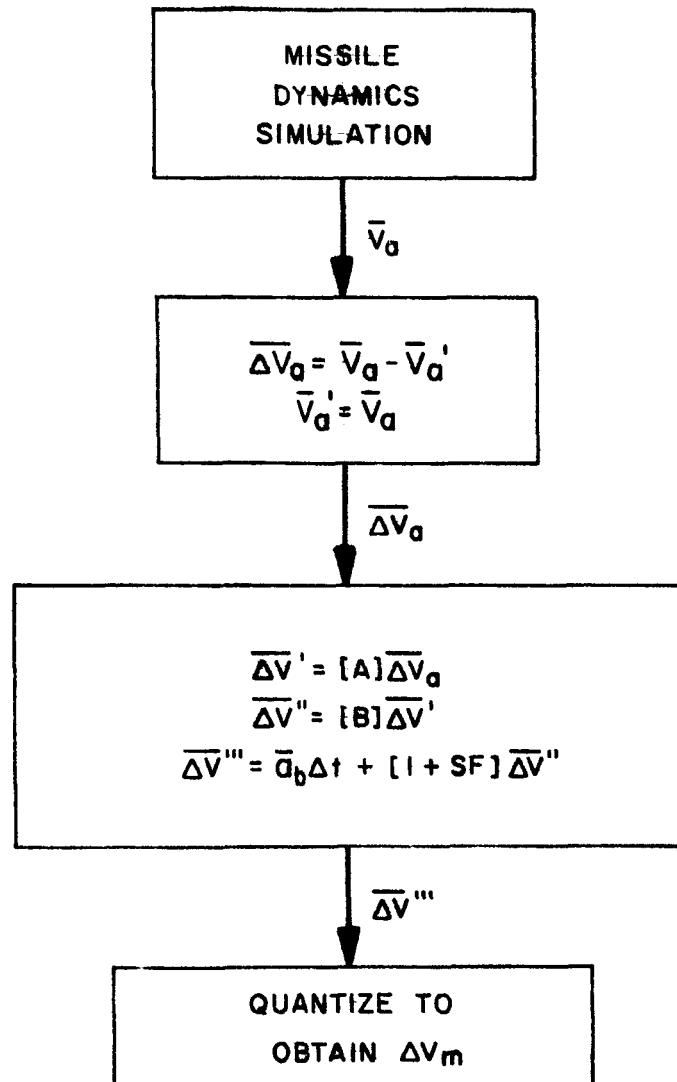


FIGURE 3
INERTIAL PLATFORM SIMULATION

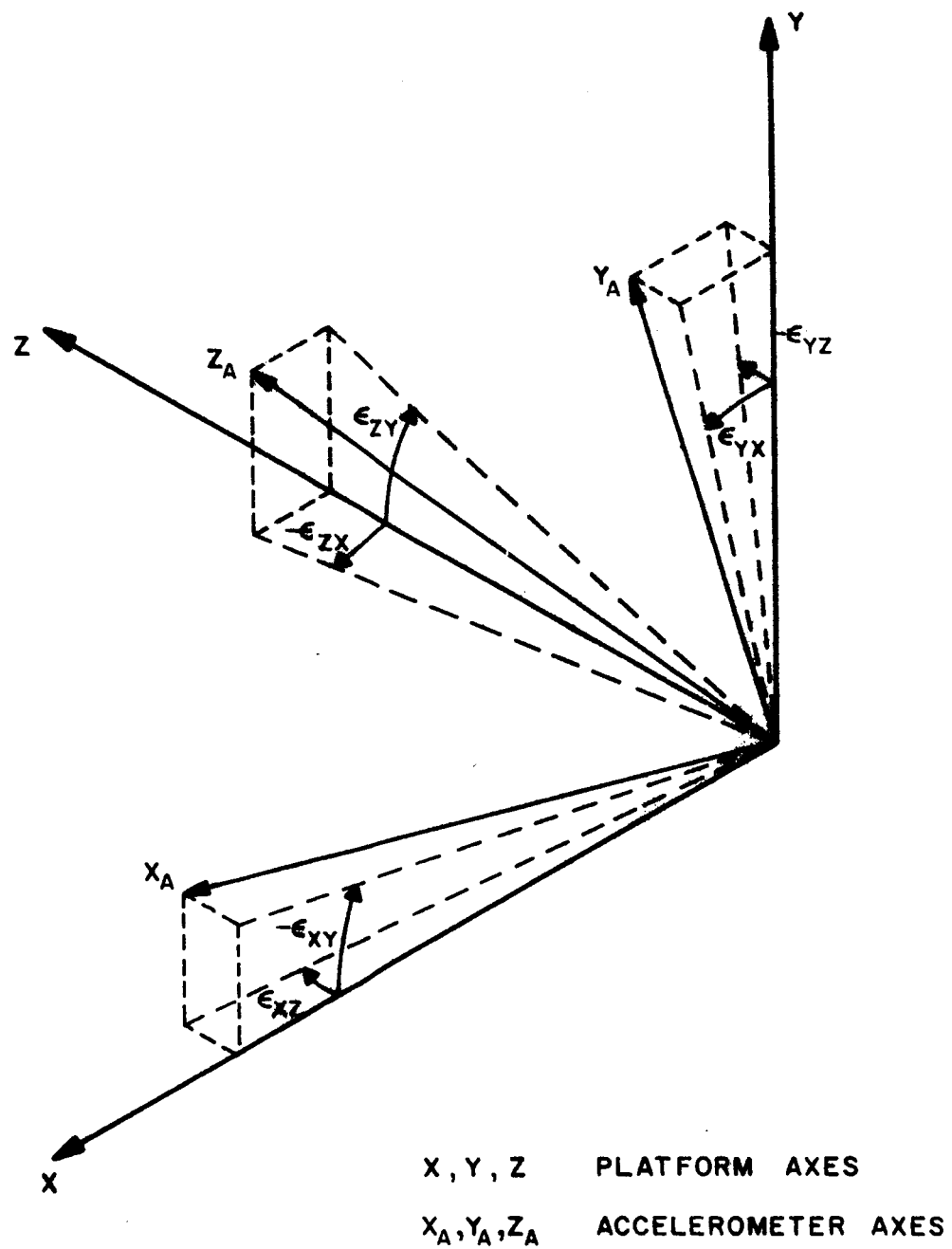


FIGURE 4
 ACCELEROMETER MISALIGNMENT

FIGURE 5
S-IVB FUEL RESERVE
V.S. S-IB FUEL LOADING

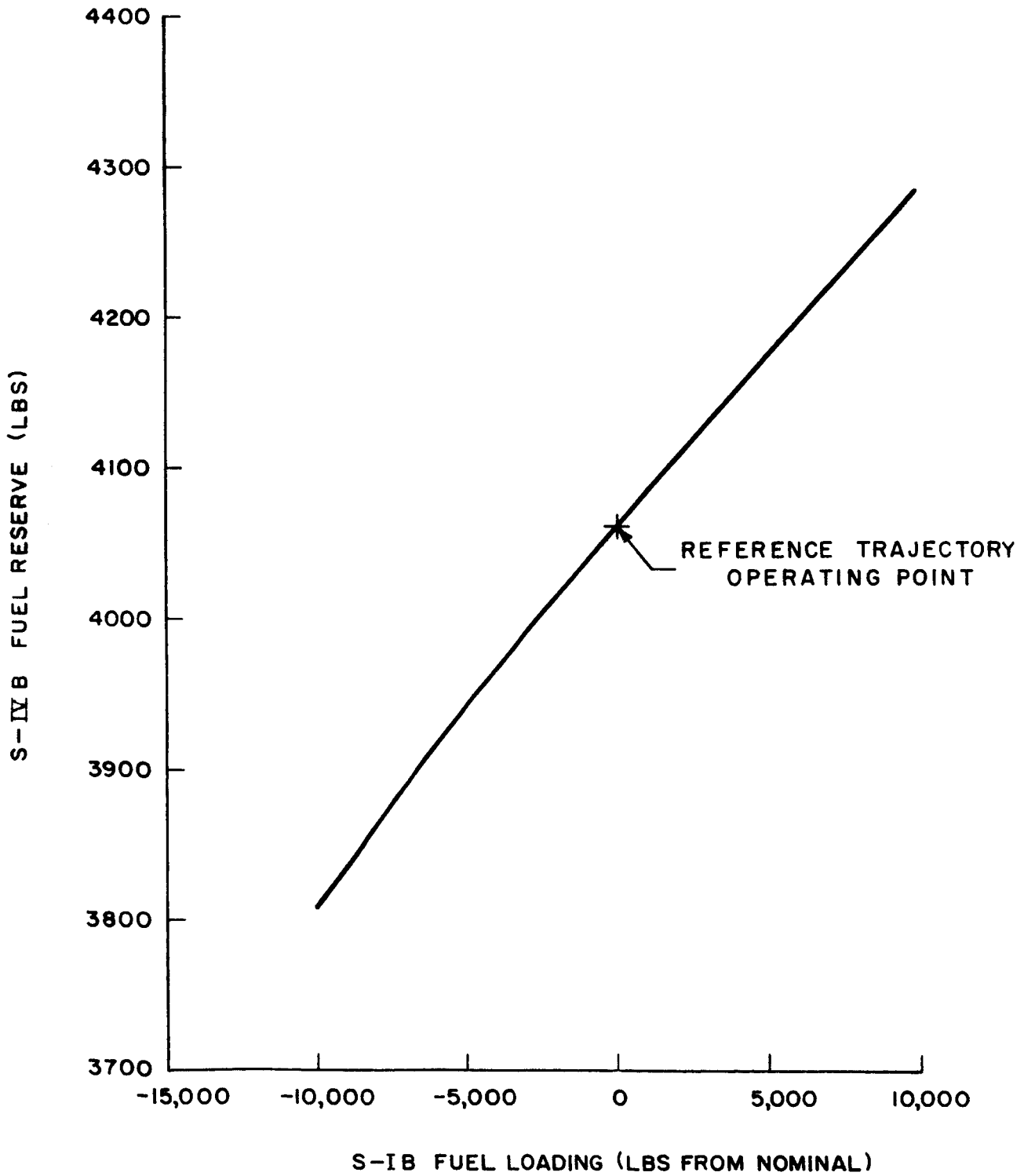


FIGURE 6
S-IV B FUEL RESERVE
V.S. S-IV B FUEL LOADING

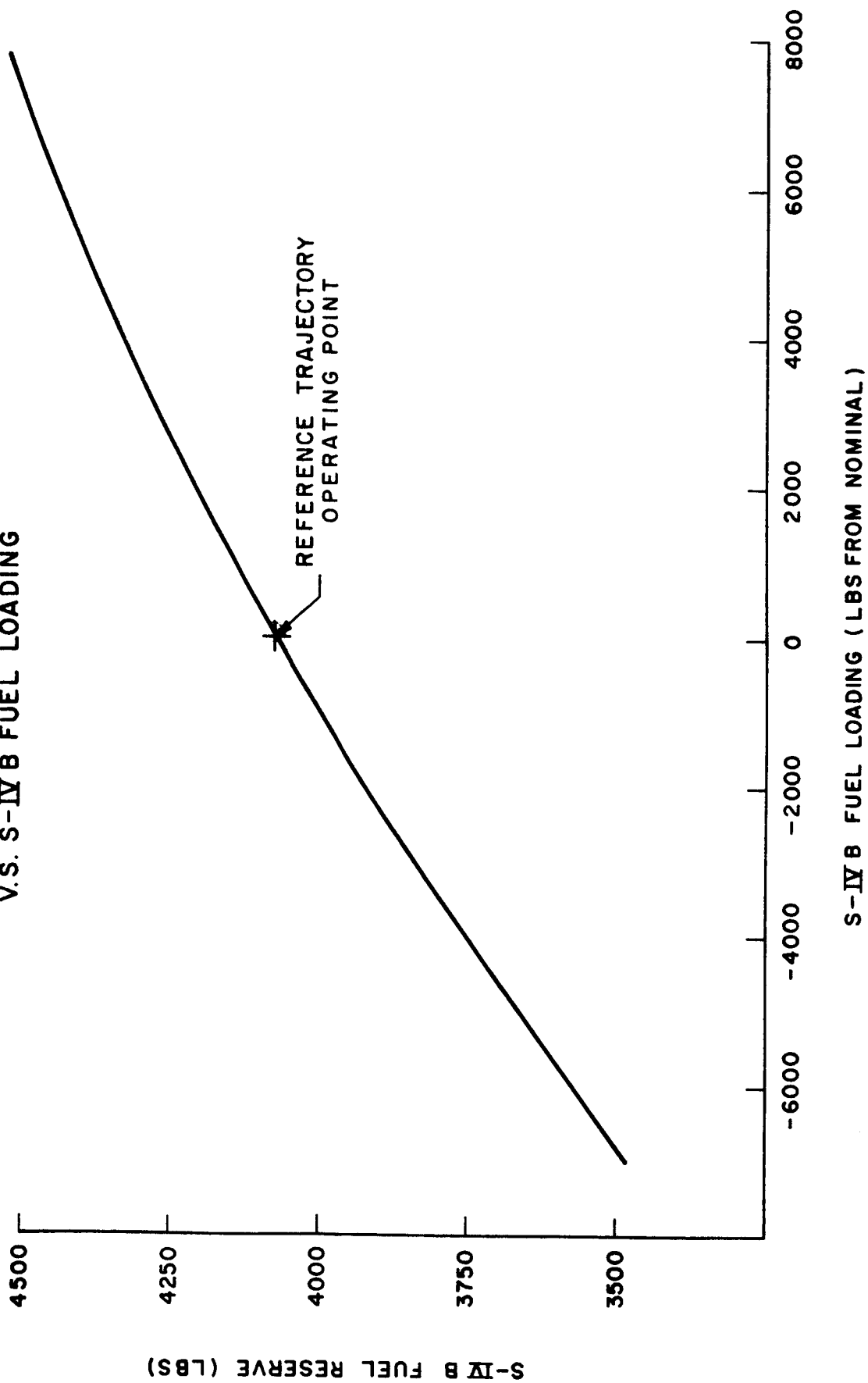


FIGURE 7
TIME OF S-IVB CUTOFF VS
ALTITUDE AT 185.4 SECONDS

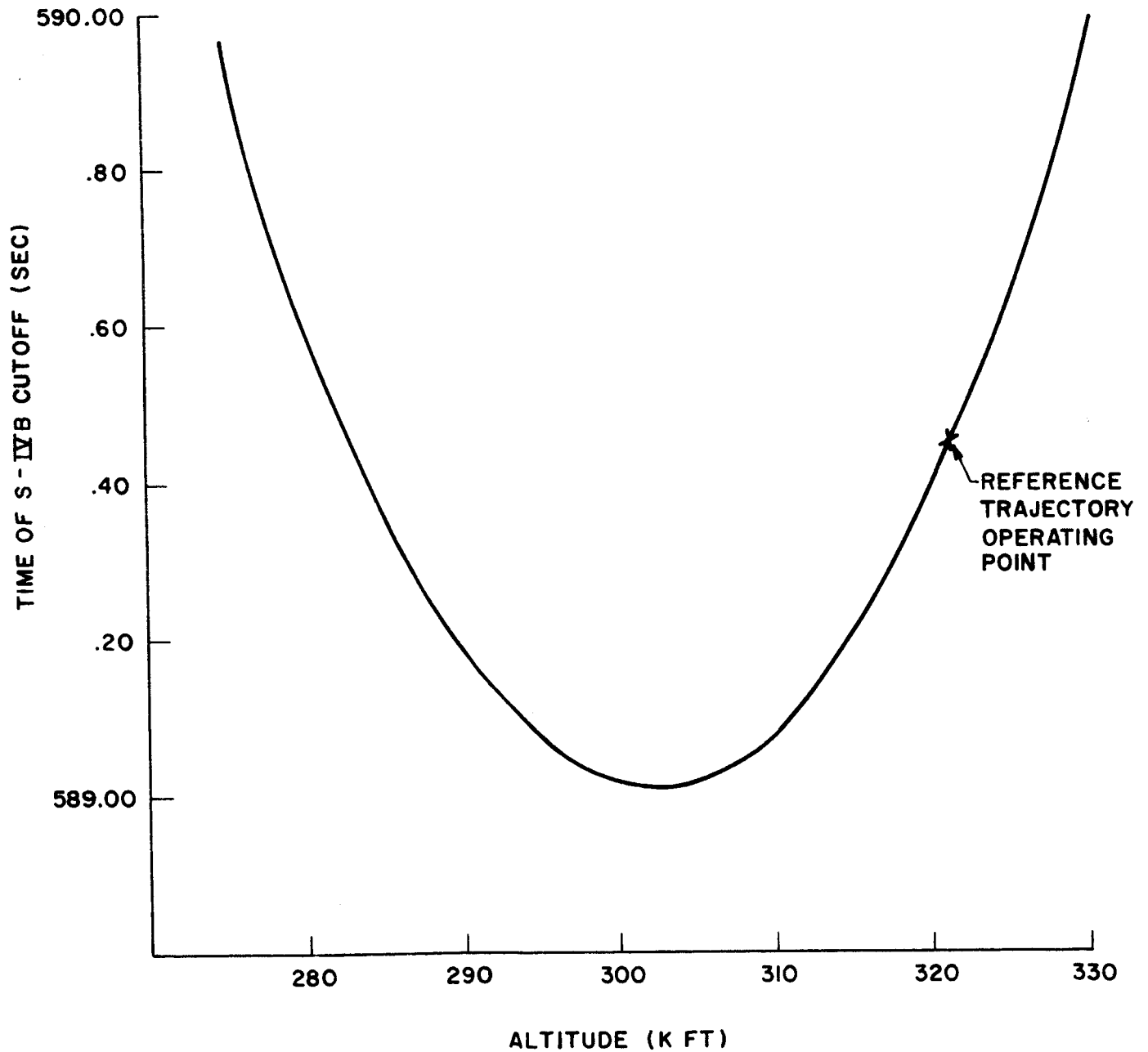


FIGURE 8
WEIGHTING SEQUENCE
OF
M/F FILTER

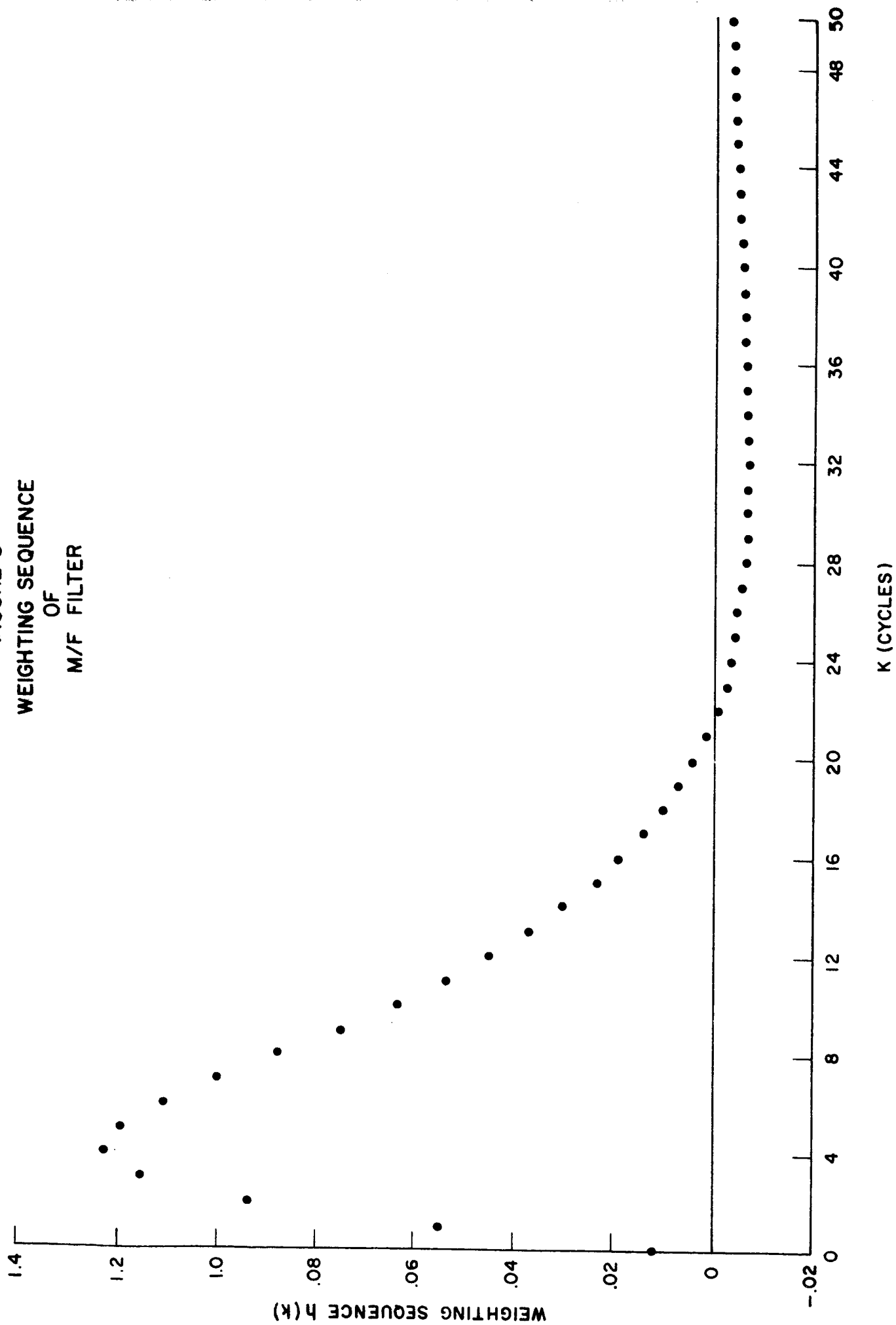


FIGURE 9
STEP RESPONSE
OF
M/F FILTER

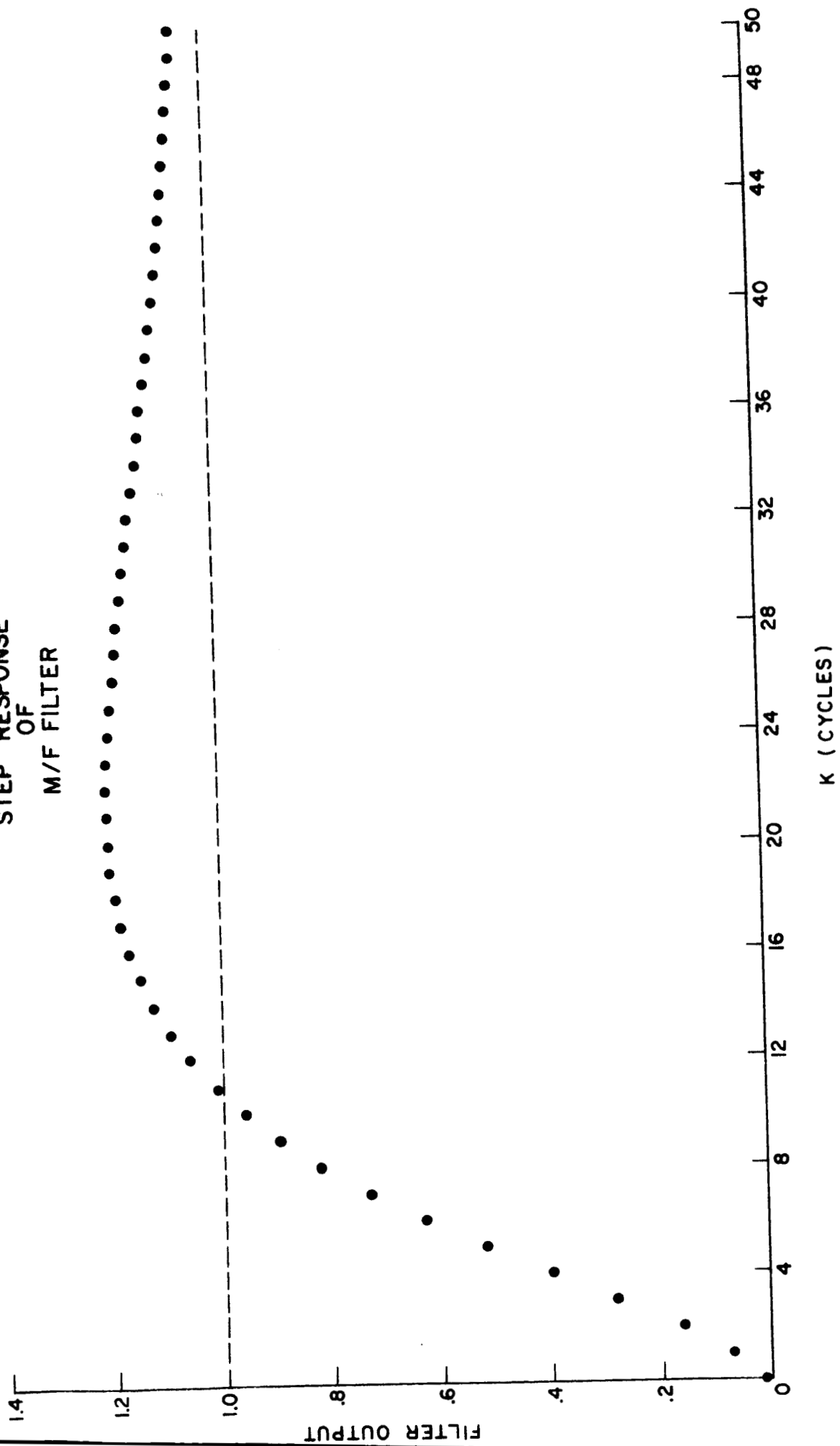
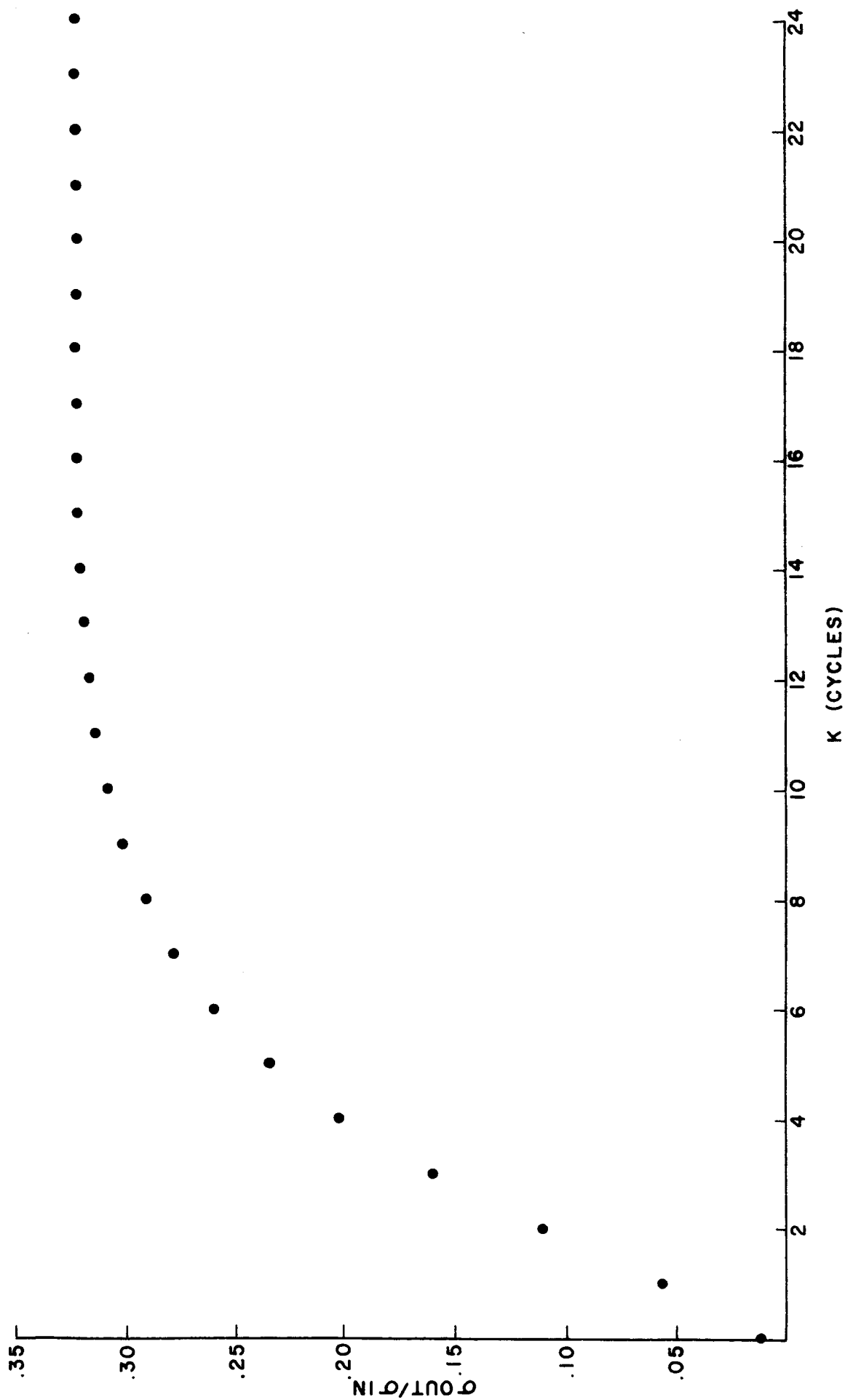


FIGURE 10
NOISE PERFORMANCE
OF M/F FILTER



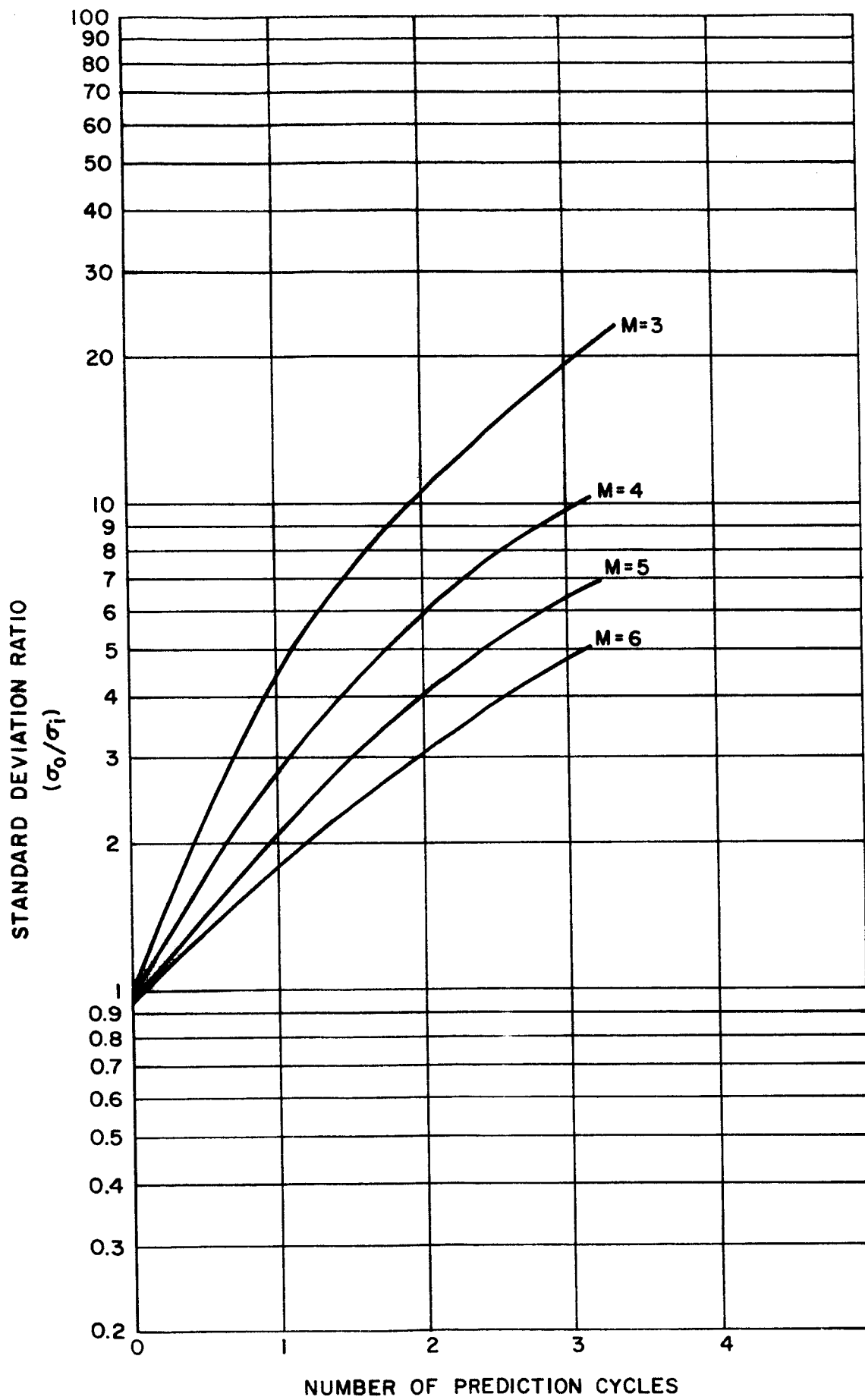


FIGURE 11

FIGURE 12

3 σ FUEL UNCERTAINTY AS A FUNCTION OF
FIRST AND SECOND STAGE I_{sp} UNCERTAINTY

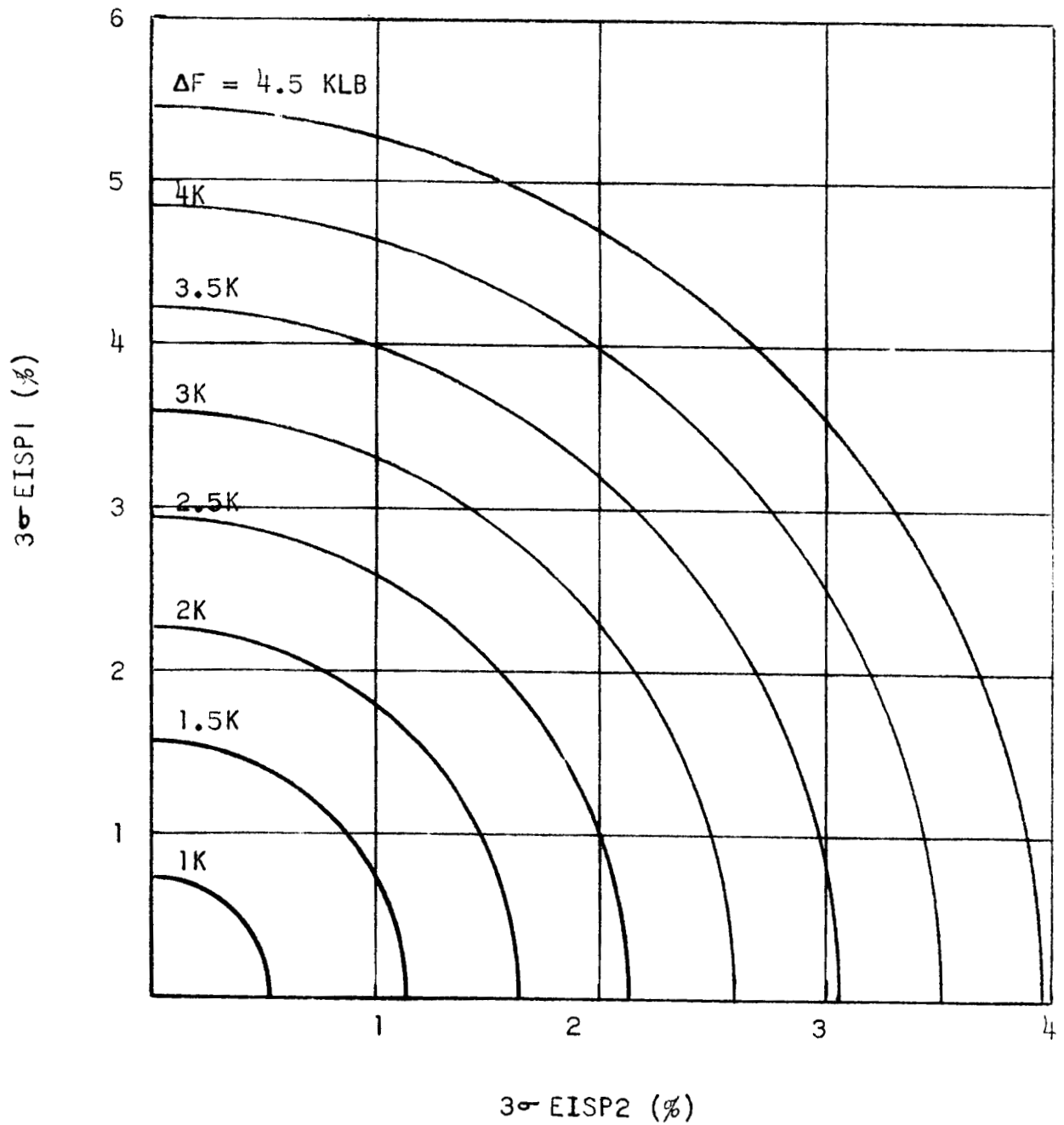


FIGURE 13
PROBABILITY OF FUEL DEPLETION AS A FUNCTION
OF FUEL RESERVE AND FUEL UNCERTAINTY

